



HAL
open science

An analytical survey of zinc white historical and modern artists' materials

Nicoletta Palladino, Mathilde Occelli, Gilles Wallez, Yvan Coquinot, Quentin Lemasson, Laurent Pichon, Slavica Stankic, Victor Etgens, Johanna Salvant

► To cite this version:

Nicoletta Palladino, Mathilde Occelli, Gilles Wallez, Yvan Coquinot, Quentin Lemasson, et al.. An analytical survey of zinc white historical and modern artists' materials. *Heritage Science*, 2024, 12 (1), pp.47. 10.1186/s40494-023-01082-4 . hal-04705882

HAL Id: hal-04705882

<https://hal.science/hal-04705882v1>

Submitted on 28 Oct 2024

HAL is a multi-disciplinary open access archive for the deposit and dissemination of scientific research documents, whether they are published or not. The documents may come from teaching and research institutions in France or abroad, or from public or private research centers.

L'archive ouverte pluridisciplinaire **HAL**, est destinée au dépôt et à la diffusion de documents scientifiques de niveau recherche, publiés ou non, émanant des établissements d'enseignement et de recherche français ou étrangers, des laboratoires publics ou privés.

RESEARCH

Open Access



An analytical survey of zinc white historical and modern artists' materials

Nicoletta Palladino^{1,2}, Mathilde Occelli³, Gilles Wallez^{1,3,4}, Yvan Coquinot¹, Quentin Lemasson^{1,5}, Laurent Pichon^{1,5}, Slavica Stankic⁶, Victor Etgens¹ and Johanna Salvant^{1,4*}

Abstract

This study is the first systematic survey of a large corpus of zinc white (ZnO) artists' materials. Zinc white is a white pigment developed within the wave of 19th-century technological developments in the paint industry. The composition, particle morphology and size, and luminescence of 49 zinc white samples from artists' materials were characterized, including three references of known synthesis methods (indirect and direct) and synthesized by the authors (ZnO nanosmoke). The corpus included historical and modern zinc white pigment powders and paint materials from the leading European and American color manufacturers. The study aims to characterize and evaluate the variability of the properties of zinc white and its paint formulations. The reference materials presented properties in agreement with the literature: indirect ZnO exhibited submicron prismatic blue-luminescent particles of higher purity than direct ZnO, which had larger acicular green-luminescent particles. ZnO nanosmoke presented acicular (tetrapod-like) blue/green-luminescent nanoparticles. Composition, particle morphology, size, and documentary sources suggested a production via the indirect method for the analyzed corpus. However, the luminescence behavior was more complex to interpret. The fundamental emission of ZnO was not always detected, even in pure ZnO powders. Three trends were identified: smaller ZnO particles for the most recent samples; green luminescence connected to larger particle size; fewer trace elements, and of the same type (i.e., lead, sulfur) for historical materials. Another interesting finding was the detection of hydrozincite in some powders, likely a degradation product of ZnO. In terms of methodology, cathodoluminescence proved a valuable tool for pigment identification. The study provides a database of zinc white references for pigment and artwork analysis.

Keywords Zinc white, Artists' materials, Painting, SEM–EDX, PIXE, XRD, Cathodoluminescence

*Correspondence:

Johanna Salvant

johanna.salvant@culture.gouv.fr

¹ Centre de Recherche et Restauration des Musées de France (C2RMF),

Palais du Louvre, Porte Des Lions, 14 Quai François Mitterrand,

75001 Paris, France

² Laboratoire Institut Photonique d'analyse Non-Destructive Européen

Des Matériaux Anciens (IPANEMA), Site du Synchrotron SOLEIL, Université

Paris-Saclay, Saint-Aubin, BP48, 91192 Gif-Sur-Yvette, France

³ UFR 926, Chimie, Sorbonne Université, 4 Place Jussieu, 75252 Paris cedex

05, France

⁴ Institut de Recherche de Chimie Paris (IRCP), UMR 8247, Chimie

ParisTech, PSL University, CNRS, 11 Rue Pierre Et Marie Curie, 75005 Paris,

France

⁵ Fédération de Recherche NewAGLAE, FR3506 CNRS/Ministère de La

Culture/Chimie ParisTech, Palais du Louvre, 75001 Paris, France

⁶ UMR 7588, Sorbonne Université, CNRS, Institut des NanoSciences de

Paris INSP, 4 Place Jussieu, 75252 Paris cedex 05, France



© The Author(s) 2023. **Open Access** This article is licensed under a Creative Commons Attribution 4.0 International License, which permits use, sharing, adaptation, distribution and reproduction in any medium or format, as long as you give appropriate credit to the original author(s) and the source, provide a link to the Creative Commons licence, and indicate if changes were made. The images or other third party material in this article are included in the article's Creative Commons licence, unless indicated otherwise in a credit line to the material. If material is not included in the article's Creative Commons licence and your intended use is not permitted by statutory regulation or exceeds the permitted use, you will need to obtain permission directly from the copyright holder. To view a copy of this licence, visit <http://creativecommons.org/licenses/by/4.0/>. The Creative Commons Public Domain Dedication waiver (<http://creativecommons.org/publicdomain/zero/1.0/>) applies to the data made available in this article, unless otherwise stated in a credit line to the data.

Journal : BMCTwo 40494	Dispatch : 10-12-2023	Pages : 31
Article No : 1082	<input type="checkbox"/> LE	<input type="checkbox"/> TYPESET
MS Code :	<input checked="" type="checkbox"/> CP	<input checked="" type="checkbox"/> DISK

25 Introduction

26 Zinc white (zinc oxide, ZnO) is a modern pigment, a
 27 product of the technological and industrial development
 28 of the 19th century. Though known since antiquity for
 29 ointments and as a sub-product in brass manufacturing,
 30 it was only at the end of the 18th century that it started
 31 to be studied as an alternative to the white par excel-
 32 lence, the toxic lead white [1]. At the time, zinc white was
 33 praised for not being a risk to human health, not dark-
 34 ening upon exposure to sulfurous gases, and for being
 35 permanent. Its covering power in oil is weaker than lead
 36 white's [2], which makes it more suitable for transparency
 37 effects and to be mixed with other pigments [3].

38 ZnO is used not only for paint materials (e.g., water-
 39 colors, oil colors, pastels, house paint, mastics, acrylics)
 40 but also as a vulcanization accelerator for rubber produc-
 41 tion, as well as for applications in ceramics, electronics,
 42 polymers, cosmetics, pharma [4] and nanotechnology
 43 [5–8]. As a pigment, it has been used as white *as-is* (in
 44 house paint and fine arts), but also for ground layers (e.g.,
 45 by Pre-Raphaelites [9] and some 20th-century American
 46 artists [10, 11]). Still commercialized today, zinc white
 47 has been widely replaced by titanium white since the sec-
 48 ond half of the 20th century and can often be found in
 49 titanium white tubes to adjust its tinting strength [12].

50 The pigment is known under different names, such as
 51 *Chinese white* (for watercolors), *snow white/Schneeweiss/*
 52 *blanc de neige, blanc de trémie, blanc léger, Constant*
 53 *white, Hubbocks white, permanent white* [1, 13].

54 It is manufactured by two main methods, both pyro-
 55 metallurgical [1]:

- 56 – The French or indirect method, ~80% of today's ZnO
 57 production [9], which uses metallic zinc as a raw
 58 material;
- 59 – The American or direct method, where zinc ores and
 60 a reducing agent (e.g., carbon coke) are heated up to
 61 reduce zinc compounds to zinc before oxidation.

62 Other methods, such as the wet chemical process, are
 63 used to produce ZnO for different applications, such as
 64 in the textile [4] and rubber industries.

65 The first successful trials of the synthesis of zinc white
 66 were performed by the chemists Jean-Baptiste Courtois
 67 (1777–1838) and Louis-Bernard Guyton de Morveau
 68 (1737–1816) in Dijon (France) around 1780 after some
 69 early tests in Germany [14]. In 1796, the English color-
 70 maker John Atkinson of Harrington issued a patent
 71 for the manufacturing of ZnO in the United Kingdom
 72 [14]. In 1834, *Winsor & Newton* first sold *Chinese white*
 73 for watercolors [15]. Large-scale production of the pig-
 74 ment for oil colors only started in the second half of the
 75 19th century, when the architectural painter Edme-Jean

76 Leclaire (1801–1872), influenced by the experiments of
 77 the French inventor Stanislas Sorel (1803–1871) [16],
 78 developed the so-called French or indirect method. He
 79 also discovered a manganese-based drier able to over-
 80 come the longer drying time of the pigment, the major
 81 drawback to its use [14].

82 Shortly after developing the indirect process, Leclaire
 83 collaborated with the leading European zinc manufac-
 84 turer, the Belgian company *Vieille Montagne*, which
 85 exploited calamine deposits, ¹ mainly in Belgium [17].
 86 The produced pigments were then sold to the main color
 87 merchants of the time, such as *Lefranc* [18], *Sennelier*²,
 88 and *Winsor & Newton* [15].

89 From the second half of the 19th century, many techno-
 90 logical developments improved pigment manufacturing
 91 (e.g., reverberatory³ and muffle/retort⁴ furnaces). How-
 92 ever, parameters such as temperature and airflow were
 93 still hard to control [19].

94 In the 1850s, the *New Jersey Zinc Company*, taking
 95 advantage of the discovery of franklinite⁵ deposits, pat-
 96 ented an alternative method of ZnO manufacturing
 97 in the United States, the so-called American or direct
 98 method. In 1892, the French process also started being
 99 used in the United States, becoming the most widespread
 100 production method of ZnO worldwide [1].

101 At the beginning of the 20th century, scientists realized
 102 that zinc white was linked to some degradation issues like
 103 chalking of house paint [20, 21] and metal soaps [22–26].
 104 These phenomena can change the visual appearance of
 105 paintings and provoke cracking, delamination, and paint
 106 loss in the most severe cases [10, 23, 24, 26, 27]. Thus,
 107 it would be important for conservators to have an easy
 108 method to identify zinc white in artworks and pinpoint
 109 early warning signals of its degradation [19].

110 A considerable amount of studies have already been
 111 performed on the interaction of zinc white with oils and
 112 the formation of metal soaps [3, 28–35], its photolumi-
 113 nescence [20, 36–40], composition [18], rheological [41]
 114 and mechanical properties [42], as well as its use and
 115 degradation in watercolors [9], oil paint [27, 43, 44] and
 116 grounds [10, 11]. Moreover, the pigment has been used
 117 for restoration since the 19th century [45]. It is still on
 118 the market today, even though many artists are unaware
 119 of its properties, use, and related degradation phenom-
 120 ena [24].

¹ Smithsonite, a zinc carbonate mineral containing some lead. 1FL01

² Personal communication. 2FL01

³ Raw materials are isolated from the fuel, but not the combustion gas. 3FL01

⁴ Heat is applied to a vessel that contains the raw materials, so that emitted
 gas and products are carried away to a separation/collection section. 4FL01
 4FL02

⁵ A mineral composed of iron, zinc, and manganese oxides. 5FL01



Fig. 1 Examples of historical zinc white samples belonging to the corpus of study: **a** *Lefranc* and *Sennelier* powders, C2RMF material collection; **b** *Lefranc* paint tube, 1930s, private collection of Nathalie Balcar (C2RMF); **c** *Grumbacher* color set, 1950s, private collection of Gilles Bastian (C2RMF); **d** *Maimeri* color chart, 1940s © Sandro Baroni, *Fondazione Maimeri*; **e** *Talens* paint tube, 1930s, private collection of Gilles Bastian (C2RMF)

121 Different types of zinc white have been identified, but
 122 as Eastaugh et al. [19] pointed out, the cause-and-effect
 123 relations of these remarks are still not completely under-
 124 stood. They tackled this issue by studying documentary
 125 sources and establishing historical synthesis patterns.
 126 Other research groups analyzed historical zinc white art-
 127 ists’ materials, focusing on specific examples, such as the
 128 French brands *Lefranc* and *Ripolin* [18, 38, 46–48].

129 Our study is the first systematic survey of a large and
 130 unique corpus of zinc white historical and modern art-
 131 ists’ materials (e.g., pigment powders, paint tubes) from
 132 Europe and the United States of America, gathered with
 133 the help of museums, cultural institutions, and research
 134 centers. This research aims to correlate the synthesis
 135 method of zinc white to its properties to identify poten-
 136 tial markers for identifying and classifying the pigment
 137 and create a reference database for painting conservation
 138 and authentication.

The corpus of samples and the methodology used
 are presented first. The results are then described and
 discussed in light of historical and modern scientific
 literature.

Materials and methods

Samples

The corpus consisted of 49 samples referred to as zinc
 white donated by museums, researchers, foundations,
 a company, or synthesized (some examples in Fig. 1). It
 covered a significant timeframe, from the end of the 19th
 century until today, even though it was impossible to date
 all the samples accurately. In this paper, the samples dat-
 ing back to the 19th–20th century are indicated as “his-
 torical”; those produced or bought in the 21st century are
 referred to as “modern”.

Table 1 below provides an overview of the samples,
 classified into three categories:

Journal : BMCTwo 40494	Dispatch : 10-12-2023	Pages : 31
Article No : 1082	<input type="checkbox"/> LE	<input type="checkbox"/> TYPESET
MS Code :	<input checked="" type="checkbox"/> CP	<input checked="" type="checkbox"/> DISK

Table 1 Summary of the samples in the corpus of analysis

Brand	Samples
Reference samples	
<i>Synthesized ZnO</i>	ZnO nanosmoke synthesized as in Zhang et al. [49]
<i>Brüggemann</i>	Two powders (2020, indirect and direct method)
ZnO manufacturers	
<i>KF chemicals</i> Japan, since 1951	One powder (historical)
<i>Kremer</i> Germany, since 1977	Two powders (2010 and 2021)
<i>Maastrichtsche zinkwit Maatschappij</i> The Netherlands, 1870–1989, then acquired by the <i>Vieille Montagne</i>	Four powders of different grades (1907–1989)
<i>Merck</i> Germany, since 1668	One powder (historical)
<i>Sikkens</i> The Netherlands, since 1792	One powder (historical)
<i>Vieille Montagne</i> Belgium, 1837–1989, then <i>Union Minière</i> , today <i>Umicore</i>	Six powders of different grades (1847–1989)
Color manufacturers	
<i>Blockx</i> Belgium, since 1865	Two paint tubes (1976 and 2021) One titan-zinc white paint tube (2021)
<i>Bocour</i> US, since 1932	One paint tube (1933–1975) One titan-zinc white paint jar (1940–1975)
<i>Charvin</i> France, since 1830	One paint tube (2010)
<i>Craftint manufacturing company</i> US, 1929–2018	One paint tube (1950s)
<i>Fezandie & Sperrle</i> US, until 1979	One powder (historical)
<i>Grumbacher</i> US, since 1905; today, in <i>Chartpark, Inc</i>	Three paint tubes (1950s and two tubes dating back to 1960–1975)
<i>Lefranc</i> France, 1720–1964, then <i>Lefranc & Bourgeois</i>	One paint tube (1930s) One paint sample (1950) One powder with a binder (before 1964)
<i>Lefranc & Bourgeois</i> France, since 1964	Two paint tubes (after 1964, 2021) One pastel (after 1964)
<i>Maireri</i> Italy, since 1923; in <i>Fila</i> group since 2014	One paint sample from a color chart (1939–1946) One paint tube (1970s)
<i>Michael harding</i> US, since 1982	One paint tube (2021)
<i>Old holland</i> The Netherlands, since 1664	One paint tube (2010)
<i>Permanent pigments</i> US, 1933–1955	One powder (1933–1955) One paint tube (1933–1955)
<i>Ripolin</i> France, since 1888	One paint sample from a color chart (1900)
<i>Sennelier</i> France, since 1887	Two powders (after 1887, 2021) Two paint tubes (after the 1920s and 2021, acrylics)
<i>Talens</i> The Netherlands, 1889–1969, then <i>Sikkens</i> group, then <i>Akzo Nobel</i>	Two paint tubes (1930s, from the same box: one in good condition, the other yellowed and dried)
<i>Vilhelm Pacht</i> Denmark, since 1887	One paint tube (1890–1909)

Brands are listed in alphabetical order. The date of production of the samples is indicated between brackets in the column on the right when available

- | | | | |
|-----|--|---|-----|
| 156 | • Reference materials of known production methods; | The samples were either in the form of powder | 159 |
| 157 | • Samples from ZnO manufacturers; | (referred to as “powder”) or of powder ground in a | 160 |
| 158 | • Samples from colormen and paint manufacturers. | binder (referred to as “paint”). Details about the analyzed | 161 |

162 samples classified by manufacturer/supplier, including
163 their product description, are available in Additional
164 file 1: Table S1.

165 **Reference materials**

166 Three modern materials, all in the form of powder and of
167 known production methods, were used as a reference for
168 the study:

- 169 • ZnO nanosmoke synthesized by the authors as
170 described in Zhang et al. [49], well-known in terms
171 of size, shape, crystallographic characteristics, optical
172 properties, point defects, and surface reactivity;
- 173 • ZnO manufactured by the German chemical com-
174 pany *Brüggemann*,⁶ either by direct or indirect
175 method.

176 Paint mockups were also prepared by grinding these
177 powders in linseed oil.

178 **Samples from ZnO manufacturers**

179 The fifteen samples from ZnO manufacturers were all
180 powders without specifications of their production
181 method. Two of them were modern materials produced
182 by *Kremer*; the remaining thirteen were historical sam-
183 ples, including different grades (*cachets or, argent, blanc,*
184 *rouge, bleu*,⁷ in order of purity) from the *Société de la*
185 *Vieille Montagne* (Liège, Belgium). Two of them (*cachets*
186 *argent, bleu*) were described by the manufacturer as “lab
187 samples”, while the other four (two *cachet blanc*, one
188 *cachet or*, and one *cachet rouge*) were from the produc-
189 tion facility *Valentin-Cocq* (Liège, Belgium). In addition,
190 samples of four different grades (*Serena witzegel, Gri-*
191 *jsegel n°3, Serena roedzegel, Serena roedzegel n°1*⁸) from
192 another historical ZnO manufacturer in the Netherlands,
193 the *Maastrichtsche zinkwit Maatschappij*, were also
194 investigated.

195 **Samples from colormen and paint manufacturers**

196 The remaining thirty-one samples of the corpus were
197 materials labeled as zinc white from a large variety of
198 colormen (~70% historical, from the end of the 19th cen-
199 tury until the 1970s, ~30% modern). Many of the leading
200 19th–20th century European and American ZnO manu-
201 facturers and colormen (e.g., *Lefranc, Sennelier, Ripolin,*
202 *Winsor & Newton, Maimeri, Grumbacher*) were repre-
203 sented (Table 1). Products from these color-makers were

204 used by the foremost 19th- and 20th-century artists,
205 whose artworks are now in different conservation states
206 [11, 22, 23, 50–55]. Paint materials were mainly paint tubes
207 except for a few samples: two fragments from *Maimeri*
208 and *Ripolin* color charts, a sample of 1950s *Lefranc* paint
209 from a canvas, and a *Lefranc & Bourgeois* pastel.

210 **Methods**

211 The corpus was analyzed by multiple techniques to shed
212 light on different properties of zinc white:

- 213 • Composition, using Scanning Electron Microscopy-
214 Energy Dispersive X-ray spectroscopy (SEM–EDX),
215 Particle-Induced X-ray Emission spectroscopy
216 (PIXE), X-Ray Diffraction (XRD);
- 217 • Particle morphology and size using optical micros-
218 copy (OM), SEM, and High angular Resolution XRD
219 (HR-XRD);
- 220 • Luminescence signature using OM under UV light,
221 cathodoluminescence (CL), and Ion Beam-Induced
222 Luminescence (IBIL);
- 223 • Binders, using Fourier-Transform InfraRed spectro-
224 scopy (FTIR).

225 Table 2 summarizes the techniques used with the
226 addressed property, sample preparation, and number of
227 analyzed samples.

228 **Optical microscopy**

229 Each sample was observed *as-is*, in the form of powder or
230 mixed with a binder, with no sample preparation. A small
231 amount was put on a microscope glass slide and observed
232 with a Nikon Eclipse LV100ND optical microscope using
233 a Nikon Xenon Power Supply XPS-100 Xenon lamp and a
234 Nikon DS-R1 camera. Three observation methods were
235 applied: dark-field mode, fluorescence mode under ultra-
236 violet (UV, 330–390 nm), and blue light (450–490 nm).

237 The NiSS-Element software was used to acquire the
238 images.

239 **Scanning electron microscopy-energy dispersive x-ray spectroscopy**

240 Two protocols were used for imaging zinc white powders
241 or paint materials.

242 The size of ZnO particles was estimated by measuring
243 about ten particles for each sample in ImageJ.
244

245 **ZnO powders**

246 The samples, previously observed using OM, were dis-
247 persed in isopropanol with the help of an ultrasonic
248 device. A drop of the dispersion was applied on a piece
249 of Si (100) attached to the sample holder by carbon tape.
250 The samples were then left to dry under a fume hood.

6FL01 ⁶ L. Brüggemann GmbH & Co. KG, Salzstraße 131, 74076 Heilbronn,
6FL02 Deutschland, <https://www.brueggemann.com/>.

7FL01 ⁷ Golden, silver, white, red, blue seals.

8FL01 ⁸ White, grey, and red seals.

Table 2 Summary of the techniques used to characterize the corpus of samples

Technique	Addressed property	Sample preparation		Studied samples ^a	
		Powder	Paint	Powder	Paint
OM under visible and UV light	Color, photoluminescence	<i>As-is</i>		All	
SEM-EDX	Particle morphology and size, elemental composition	Dispersed in ethanol and dried on a Si wafer		Cross-section	20 10
PIXE	Elemental composition, trace elements	Between polypropylene sheets			19 22
XRD	Crystalline structure, composition, particle size ^b	<i>As-is</i> for micro-XRD; in borosilicate capillaries for HR-XRD			22 23
CL	Cathodoluminescence	Mixed with araldite and spread on a roughened glass slide	Cross-section	19	15
FTIR	Type of binder, presence of metal soaps, and other compounds	<i>As-is</i>		12	18

^a Detailed in Additional file 2: Table S2.0

^b High-angular Resolution X-Ray Diffraction at the ESRF

251 The methodology was developed on reference powder samples (i.e., *Brüggemann* ZnO, indirect and direct) 252 using a FEG SUPRA 40 ZEISS at the *Institut des Nano-Sciences de Paris* (INSP; Paris, France); the other powder 253 samples were observed using a FEG Supra55VP ZEISS at the IPANEMA laboratory (Gif-sur-Yvette, France). 254

255 The InLens detector (secondary electrons) acquired the images at an operating voltage of 5 kV and a 3–4 mm 256 working distance. 257

260 **Zinc white samples with binder**

261 Samples containing a binder were embedded in araldite, as explained below for cathodoluminescence. The cross- 262 sections were polished up to 1 μm and sputter-coated with 0.7 nm of platinum for analysis with a Jeol JFC- 263 2300HR fine coater. Images and analyses were conducted using a JEOL 7800F with two SDD Bruker AXS 6|30 264 detectors at the *Centre de Recherche et Restauration des Musées de France* (C2RMF; Paris, France). The images 265 were acquired using secondary (SE) and backscattered electrons (BSE) at an operating voltage of 5 kV and a 266 working distance of 6 mm. 267

268 EDX analyses were performed at an operating voltage of 15 kV and an optimal working distance of 9.5 mm. 269 6–12 points were selected based on the BSE images obtained at ×10 000 magnification. The software Esprit 270 (Bruker, version 2.3) acquired and stored data. 271

277 **Particle-induced X-ray emission spectroscopy and Ion Beam-Induced Luminescence**

278 The samples were mounted between two polypropylene sheets (FLUXANA) of 6 μm thickness at a 2–3 mm distance to the extracted beam. 279 280 281

The analyses were performed at the *Accélérateur Grand Louvre d'Analyses Élémentaires* (NewAGLAE, ANR-10-EQPX-22) [54]. Four Peltier-cooled SDD detectors were used: one for low energies with a helium flux (1–10 keV), placed at 50° relative to the beam axis, three for high energies, at a relative angle of 45° (1 with a 200 μm Al filter, 2 with 25 μm Co filter) [49]. Two areas of 1000 × 1000 μm² with a pixel size of 50 × 50 μm² were measured for each sample, with a 100,000 total dose (corresponding to a charge of 0.8 μC) using a 3 MeV proton beam. 282 283 284 285 286 287 288 289 290 291

The used standards were DRN for calibrating the low-energy detector and two copper-based standards, BS938 and CTIF6, for the high-energy detectors. 292 293 294

Sample luminescence was collected by a 1 mm diameter optical fiber placed at 45° to the beam axis, conducted to a research grade OCEAN OPTICS QE65000 spectrometer. It was measured in the wavelength range 200–1000 nm, with a resolution of 3 nm FWHM (100 μm entrance slit) [56]. 295 296 297 298 299 300

X-Ray diffraction

Micro-XRD No specific sample preparation was required; ZnO powders or paint fragments were put *as-is* on the sample holder. 301 302 303 304

The experimental setup consisted of a XENOCs GENIX 3D copper source with a high-brilliance X-ray tube (power of 30 W, diameter of 30 μm) and Xenocs FOX 3D optics, which delivers a beam at the length of 1.5418 Å (Cu Kα1-2), at 50 kV, 600 μA, with a pixel size resolution of 200 μm. The diffraction patterns were acquired by a Rigaku R AXIS IV + + imaging plate detector developed by Bede Scientific Instruments Limited. 305 306 307 308 309 310 311 312

313 The analyses were carried out at an angle of incidence of
314 about 10°.

315 The acquired 2D data was transformed into a diffrac-
316 togram by the FIT2D software; crystalline phases were
317 identified by the software QualX 2.0 [57].

318 *High angular resolution-X-Ray diffraction* A selection of
319 samples was analyzed at the ID22 beamline at the Euro-
320 pean Synchrotron Radiation Facility (ESRF) [58–61].
321 Analyses were performed on samples in borosilicate cap-
322 illaries ($\phi=0.5$ mm, WJM-Glas/Müller GmbH); a LaB₆
323 standard was used as a reference for instrumental resolu-
324 tion.

325 Measurements were performed at $\lambda=0.3542$ Å
326 (35 keV), thanks to the new Extremely Brilliant Source
327 with a highly monochromatic beam of about 1×1 mm²
328 and low divergence. Diffracted photons were measured
329 by scanning the 2θ circle over the 0–43° range holding an
330 EIGER2 2 M-W CdTe pixel detector positioned behind
331 thirteen Si (111) analyzer crystals.

332 A preliminary identification of the present phases was
333 performed using the software QualX mentioned above.
334 A Williamson-Hall analysis was performed by fitting the
335 diffraction peaks through the software WinPLOTR [62]
336 of the FullProf Suite to calculate the average size of the
337 ZnO crystallite in and perpendicular to the (001) plane,
338 the aspect ratio, and the lattice strain of the crystallites,
339 by taking into account the broadening of the diffraction
340 peaks. Details about the procedures are available in the
341 Additional file 1.

342 **Cathodoluminescence**

343 All the samples were embedded in araldite 2020 trans-
344 parent liquid adhesive epoxy (volume ratio epoxy adhe-
345 sive/catalyzer of 10:3) to avoid any luminescence from
346 the resin, according to the following protocols:

- 347 • For ZnO powders, a small amount of sample was
348 mixed with the araldite and applied on a roughened
349 microscope glass slide. The resulting slides were
350 lightly polished with a 1200 grit SiC disc by Buehler
351 (15 μ m) to obtain a flat surface;
- 352 • For zinc white samples containing a binder, small
353 paint flakes were embedded in araldite. The molded
354 samples were sliced to obtain two cross-sections and
355 then polished.

356 Experimental conditions were fixed at an operating
357 voltage of 11 kV and a current of ~ 390 μ A.

358 The cathodoluminescence system Cambridge Imag-
359 ing Technology Ltd CL8200 Mk5-1, consisting of a
360 controlled electronics unit and a vacuum chamber
361 associated with an electron gun, was used to study

the cathodoluminescence of the samples. Images were
acquired with an Olympus BH-2 optical microscope
(10 \times objective). The exposure conditions were fixed at
3 s with a gain of 5.1x, slightly adjusted for some samples
to avoid overexposed images. A Nikon DS-Ri2 camera
and the NiSS-Element software were used to acquire and
store the images.

An Ocean Optics QE65000 spectrometer acquired
luminescence spectra; four accumulated spectra were
recorded by the Ocean Optics SpectraSuite software with
an exposure of 2 s. The two main luminescence peaks'
position, intensity, and width were noted.

Fourier-transform infraRed spectroscopy

No sample preparation was required; a small amount of
material was directly placed on the accessory before each
measurement.

Samples were analyzed using an FT-IR Frontier Perkin-
Elmer Spectrometer with an MCT detector. An ATR
Goldengate accessory from Specac with a diamond tip
or a diamond anvil cell from High-Pressure Diamond
Optics, Inc. was used for the measurements, depending
on the sample amount available. Spectra were collected
in the 4000–400 cm⁻¹ range with a resolution of 4 cm⁻¹
and an accumulation of twenty (ATR Goldengate acces-
sory) or forty (diamond anvil cell) spectra.

Data were acquired and processed using the software
Spectrum (PerkinElmer).

Results

This section consists of three parts: results about the
composition of the samples are presented first, followed
by insights on morphology and size of ZnO particles,
and, finally, luminescence properties. An overview of the
findings for each sample is provided in Table 3; detailed
results per analytical technique are available in Addi-
tional file 2: Table S2.

Composition

After a short presentation of the results on the binders,
the identified inorganic phases composing the samples
are described: the purity and formulations of the ZnO
materials are shown first, with major and minor com-
pounds found, followed by the detected trace elements.

Binders⁹

FTIR analyses confirmed that all the analyzed paint
samples contain oil-based binders except for the *Perma-
nent Pigments* watercolor tube, made of gum arabic. The

⁹ Zinc carboxylates were found in all the analyzed paint materials.

Table 3 Synthesis of the analytical results obtained on the studied samples




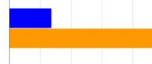


Sample	Date	wt % ZnO ^a	Other main compounds ^b	Trace elements ^c	Morphology ^d	Size (nm)	Luminescence under UV	Cathodoluminescence
Reference samples								
<i>Brüggemann direct</i>	2020	99.7	-	S, Cl, Ca, Fe	Mostly acicular	Large 	Green	Green
<i>Brüggemann indirect</i>	2020	100.0	-	Fe, Ni	Prisms	Small 	Some green grains	Blue
ZnO nanosmoke	2021	99.9	-	Fe	Acicular	Small 	Green with few green grains	Blue
ZnO manufacturers								
<i>KF Chemicals</i>	-	95.1	Hydrozincite	Pb, Fe, Ni	Prisms	Small 	Green	Green
<i>Kremer 2010</i>	2010	94.7	Hydrozincite	Ni, Fe	Prisms	Small 	Green with green and blue grains	Blue
<i>Kremer 2021</i>	2021	99.8	-	Ca, Cl, Fe	Prisms	Small	Green with blue grains	Blue
<i>Maastrichtse zinkwit Grijszegel n°3</i>	1907 - 1989	Y	Hydrozincite	N/A	N/A	N/A	Orange	Light green
<i>Maastrichtse zinkwit Serena roedzegel</i>	1907 - 1989	93.8	Hydrozincite	S, Pb, Fe, Ni	Prisms	Small 	Green	N/A

Table 3 (continued)

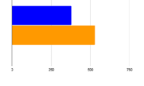
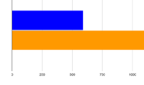
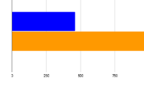
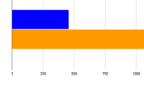
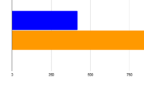
Maastrichtsc he zinkwit Serena roedzege n°1	1907 - 1989	Y	Hydrozincit e	N/A	Prisms	Large	Orange	Light green with blue grains
Maastrichtsc he zinkwit Serena witzegel	1907 - 1989	Y	Hydrozincit e	N/A	Prisms	Small	Orange	Blue with green grains
Merck	-	92.5	Hydrozincit e	Ni	Prisms, acicular	Large 	Green with green grains	Blue-green
VM cachet argent, lab	1847 - 1989	99.9	-	Pb, Fe	Prisms	N/A	Green with green and blue grains	Blue-green
VM ^f cachet bleu, lab	1847 - 1989	99.7	-	Pb, S, Fe	Prisms	Medium 	Green with green grains	Green
VM ^f cachet blanc, MNF190	1847 - 1989	99.0	Hydrozincit e	-	Prisms, acicular	Large 	Green with green and blue grains	Blue-green
VM ^f cachet blanc, MNF193	1847 - 1989	99.8	-	Pb, S, Fe	Prisms, acicular	Large	Green	Green
VM ^f cachet or	1847 - 1989	98.9	Hydrozincit e	Pb, S, Fe, Ni	Acicular , prisms	Large 	Green with green and blue grains	Green
VM ^f cachet rouge	1847 - 1989	99.1	Hydrozincit e	Pb, S, Fe	Prisms, acicular	Large 	Green with green grains	Green
Color manufacturers								
Blockx paint tube	2021	99.8	-	Pb, Fe, Ti, Ni	N/A	N/A	Green	N/A
Blockx, titan- zinc white	2021	68.4	TiO ₂	Al, Si, Pb, Cl, Fe, Ca	N/A	N/A	Blue	N/A

Table 3 (continued)



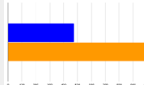
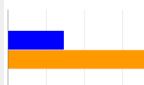
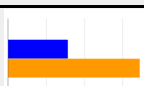
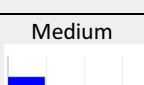
paint tube									
<i>Bocour</i> paint tube	1933 - 1975	73.9	BaSO ₄	Sr, Ni	N/A	N/A		Green and blue with green grains	Blue with green grains
<i>Charvin</i> paint tube	2010	63.6	CaCO ₃	Si, Ti, Mg, Fe, Zr	N/A		Blue with blue and green grains	N/A	
<i>Craftint Manufacturing Company</i> paint tube	1950s	99.5	-	Ti, Al, S, Fe, Cl, Ni	Prisms	Small	Green with a few green and blue grains	Light blue	
<i>Fezandie & Sperrle</i>	1850 - 1979	99.6	-	Pb, S, Cd, Ni	Prisms	Medium ^g 	Green with green grains	Green	
<i>Grumbacher</i> pre-tested paint tube	1950s	99.5	-	Pb, Ni, Al	N/A	N/A	Green with green and blue grains	Blue with green and blue grains	
<i>Grumbacher Gainsbourou</i> gh paint tube	1960 - 1975	99.8	-	Al, Ti, Ni	N/A	N/A	Green	Blue with green grains	
<i>Grumbacher</i> pre-tested, paint tube	1960 - 1975	99.4	-	Si, Al, Ca, Fe, Ni	N/A	N/A	Green	Blue with green grains	
<i>Lefranc</i> paint tube	1930s	99.4	-	Pb, Al, S, Fe, Ca, Ni	N/A		Green and blue with green grains	Green	
<i>Lefranc</i> paint sample	1950	Y	-	N/A	N/A		Light green	N/A	
<i>Lefranc</i> powder with binder	1850 - 1964	90.5	SiO ₂	Ca, Fe	N/A		Green with green grains	N/A	
<i>Lefranc & Bourgeois</i> paint tube	after 1964	99.4	-	Ti, Al, Ca, Fe, Cl	Prisms	Medium 	Blue with green and blue grains	Blue	
<i>Lefranc &</i>	2021	99.8	-	Cl, Fe, Ni	Prisms	Small	Green with	Blue with	

Table 3 (continued)


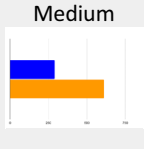
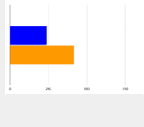
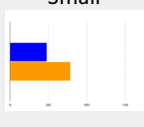
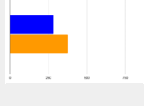
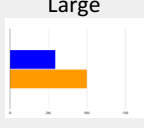
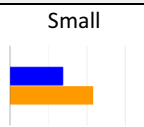
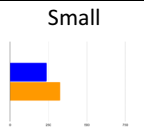
<i>Bourgeois</i> modern paint tube							green and blue grains	green grains
<i>Lefranc & Bourgeois</i> pastel	after 1964	99.3	-	Pb, S, Cl, Ni, Fe	N/A	Medium 	Green with a few green grains	N/A
<i>Maimeri</i> color chart	1939 - 1946	60.4	BaSO ₄ , CaCO ₃ , ZnS	Sr, Ni, Fe	N/A		Green with green grains	N/A
<i>Maimeri</i> paint tube	1970s	59.2	BaSO ₄ , CaCO ₃ , ZnS	Sr, Fe, Ni	Prisms	Small 	Green	Light blue
<i>Michael Harding</i> paint tube	2021	99.8	-	Fe, Ni	N/A	N/A	Green with blue grains	N/A
<i>Old Holland</i> paint tube	2010	94.0	TiO ₂	Si, Al, Fe, Ni	N/A		Blue	N/A
<i>Permanent Pigments</i> watercolor paint tube	1933 - 1955	95.2	Pb	K, Ca, Si, Fe, Ni	N/A	N/A	Green with green, blue grains	Blue with green grains
<i>Ripolin</i> color chart	1900	Y	-	N/A	Prisms, acicular	Large 	Green with green grains	Green with green grains
<i>Sennelier</i>	after 1887	99.9	-	Fe, Ni	Prisms	Small 	Green with a few blue grains	Green
<i>Sennelier</i>	2021	99.9	-	S, Fe, Ni	Prisms	Small 	Green with blue grains	N/A
<i>Sennelier</i> paint tube	after 1920s	60.0	Ba, TiO ₂ , SiO ₂	Al, Ca, Zr	N/A	N/A	Green with blue and green grains	N/A
<i>Sennelier</i>	2021	Y	BaSO ₄	N/A	N/A	N/A	Green with	N/A

Table 3 (continued)

acrylics paint tube							blue and green grains	
<i>Talens</i> paint tube	1930s	99.8	-	S, Pb, Ca, Ni	Acicular, prisms	Large 	Green with green grains	Light blue
<i>Talens</i> paint tube (dried)	1930s	99.8	-	S, Pb, Fe	N/A		Green and blue with green grains	Light blue
<i>Vilhelm Pacht</i> paint tube	1890 - 1909	98.2	-	Si, Al, Cl, Sn, Fe, S, Ca, K, Pb, Zr, Ni	Prisms	Small 	Green and blue with green grains	Light blue
Samples of different compositions than zinc white								
<i>Blockx</i> paint tube	1976	1.1	Pb (91.3 wt%), Sn, Cl	N/A	N/A	N/A	N/A	N/A
<i>Bocour</i> titan-zinc white paint jar	1940 - 1975	3.3	SiO ₂ (38.1 wt%), CaCO ₃ , TiO ₂ , BaSO ₄ , ZnS, K	N/A	N/A	N/A	N/A	N/A
<i>Permanent Pigments</i>	1933 - 1955	0.0	TiO ₂ (99.9 wt%)	N/A	N/A	N/A	N/A	N/A
<i>Sikkens</i>	-	Y?	Hydrozincite ^e , Pb	N/A	N/A	N/A	Orange	Blue with a few green grains

White background for samples in the form of powder, gray for samples in the form of paint. N/A indicates that the analysis was not performed

^a From PIXE and XRD. When no PIXE was available an "Y" indicated the presence of ZnO

^b 1-10 wt%, listed in decreasing order; from PIXE and XRD

^c < 1 wt%, listed in decreasing order; from PIXE

^d From SEM

^e Classification from SEM data (small if both diameter and lengths < 500 nm; medium if at least one dimension > 500 nm; large if at least one dimension > 1000 nm); numerical values from Williamson-Hall analysis (HR-XRD data): in blue the estimated length along (hk0), in orange the estimated length along (00 l); the indicated maximum is 1000 nm, apart from larger particles (i.e., *KF Chemicals*; *VM cachet bleu, blanc et or*; *Lefranc paint tube*)

^f *Vieille Montagne*

^g 73.9 wt% Zn calculated by PIXE. XRD and FTIR revealed that the sample is mostly made of hydrozincite

407 *Lefranc & Bourgeois* pastel had an oil binder. The *Lefranc*
408 powder contained some wax.

409 **Inorganic phase(s) of zinc white materials**

410 The inorganic phases of the samples were studied using
411 a combination of results from PIXE and XRD analyses.

PIXE measurements were used to quantify the amount
of the significant mineral phases composing the samples
and trace elements. The results were expressed in weight
percent (wt%). XRD allowed the identification of the
crystalline phases of the samples.

412
413
414
415
416

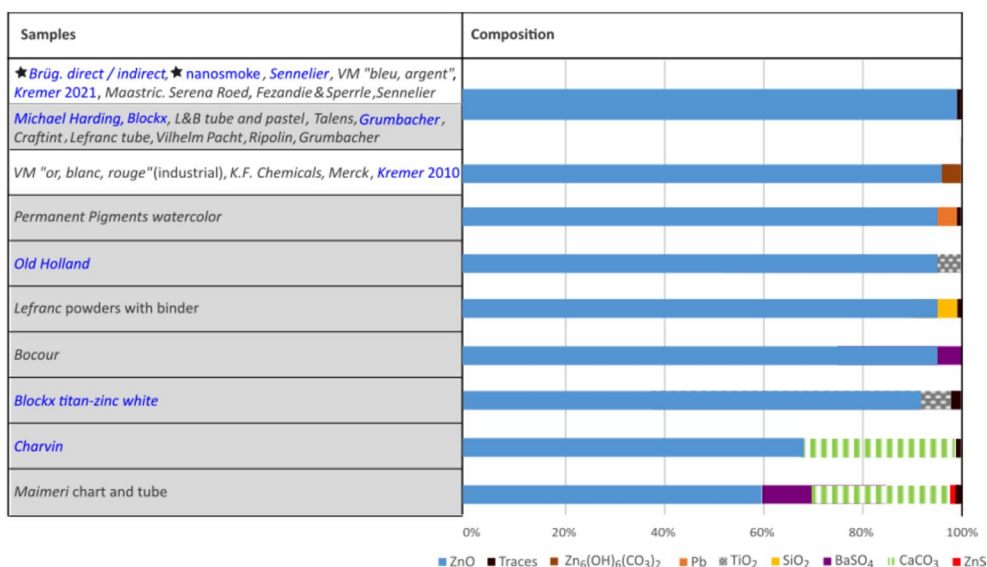


Fig. 2 Composition of the zinc white samples belonging to the corpus of the study. Reference samples are indicated with a star; in blue are modern samples, and in black are historical ones. White background for samples in the form of powder, gray for samples in the form of paint

417 *Purity and formulations of zinc white materials* The
 418 amount of ZnO (in wt%) detected for each sample investi-
 419 gated by PIXE is indicated in Table 3.

420 As shown in Fig. 2, most of the analyzed samples were
 421 almost pure ZnO (>98 wt%), in particular the powder
 422 samples (including the three reference materials).

423 The only exceptions were ten powders containing
 424 hydrozincite (Zn₅(CO₃)₂(OH)₆), identified by XRD¹⁰ and
 425 FTIR. In particular, the compound was found in the 2010
 426 Kremer ZnO powder, while it was not detected on the
 427 very same powder back in 2010 with the same setup; the
 428 Kremer ZnO powder purchased in 2021 did not contain
 429 hydrozincite either. These results suggest that the com-
 430 pound formed over time, probably from converting ZnO
 431 upon exposure to air [38, 63]. Interestingly, it was found
 432 only in industrial *Vieille Montagne* samples, not in the
 433 ones referred to by the company as “lab samples”.

434 The *Sikkens* powder, mostly hydrozincite with some
 435 lead-based compound and likely some ZnO, represents a
 436 peculiar case. An FTIR spectrum of the sample is avail-
 437 able in the Additional file 1: Figure S1.

438 Over half of the paint samples were almost exclusively
 439 made of ZnO (>98 wt%, Fig. 2, Table 3). Though usually
 440 not mentioned on the product label, the rest of the cor-
 441 pus contained significant amounts of other compounds
 442 (4–35 wt%) such as titanium dioxide (TiO₂), calcium car-
 443 bonate (CaCO₃), barium sulfate (BaSO₄), quartz (SiO₂)
 444 and lead-based compounds (Fig. 2).

445 Interestingly, four samples branded as zinc white¹¹
 446 proved to be made out of entirely other compounds than
 447 ZnO. This is possibly evidence of adulteration, a common
 448 issue for artists’ materials, particularly zinc white, in the
 449 19th century, as the recurrence of the topic in painting
 450 treatises of the time shows [64, 65]. Those samples, listed
 451 at the bottom of Table 3, were not investigated further in
 452 this study; only the *Sikkens* powder mentioned above was
 453 investigated further due to the detection of hydrozincite.

454 *Trace elements* Several elements were detected as traces
 455 (<1 wt%) by PIXE in both powders and paints: iron,
 456 nickel, lead, sulfur, calcium, aluminum, chlorine, silicon,
 457 titanium, strontium, potassium, zirconium, magnesium,
 458 tin, and cadmium (Fig. 3).

459 Iron and nickel were detected in almost all samples,
 460 with values usually lower than 0.1 wt%. Iron is likely
 461 ascribed to contamination, while the detection of nickel
 462 may be related to the PIXE detector. Lead and sulfur were
 463 present in about half of the analyzed samples, almost
 464 exclusively historical; calcium, aluminum, and chlorine
 465 were found in about a third of the analyzed samples,
 466 mostly paint materials, while others were found sporadi-
 467 cally. For example, cadmium traces were detected only in
 468 the *Fezandie & Sperrle* zinc white powder and might be

¹¹ A *Blockx* paint tube, lead-based; *Sikkens* powders, mostly made of hydro-
 zincite with ZnO and some lead-based minor compound; *Permanent Pig-*
ments powders, titanium white; a titanium-zinc white jar, a mixture of
 CaCO₃, BaSO₄, TiO₂, quartz with ZnS and ZnO as minor compounds.

¹⁰ HR-XRD used for the quantification, when available.

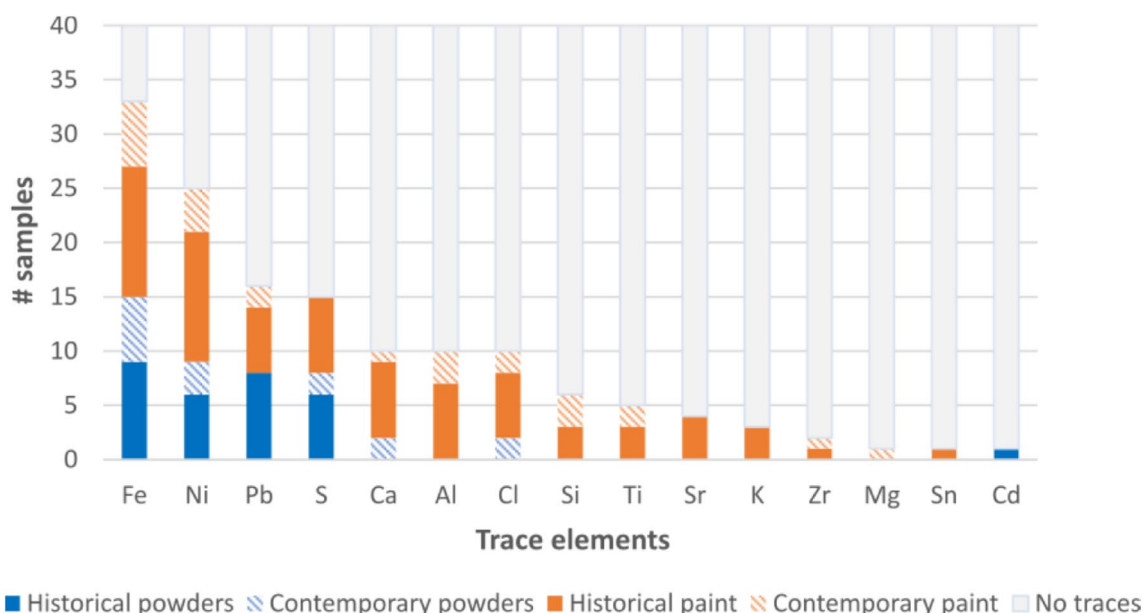


Fig. 3 Trace elements in zinc white samples belonging to the corpus of the study analyzed by PIXE

469 related to European zinc ores, as underlined by Holley
470 [66].

471 Looking at reference samples, *Brüggemann* indirect
472 and ZnO nanosmoke powders were the purest of the
473 corpus, with no traces other than iron and nickel (about
474 200–500 ppm in total). *Brüggemann* direct ZnO was less
475 pure regarding amount (~3200 ppm) and type of trace
476 elements (i.e., sulfur, chlorine, calcium, and iron). The
477 *Sennelier* powder stood for its extreme purity (less than
478 2000 ppm of trace elements).

479 Some trace elements were only detected in paint materi-
480 als (i.e., aluminum, silicon, titanium, strontium, potas-
481 sium, zirconium, magnesium, and tin; Fig. 3). Aluminum
482 may come from aluminum stearates, a standard paint sta-
483 bilizer, or aluminum silicates when detected with silicon
484 (i.e., *Grumbacher*, *Vilhelm Pacht*, *Old Holland*, *Blockx*
485 *Ti-Zn* white). Strontium likely originated from calcium
486 carbonate or barium sulfate since it is a common impu-
487 rity of the natural form of barium sulfate [1, 67] and was
488 only detected in samples containing these compounds
489 (e.g., *Maimeri*). Magnesium might come from magne-
490 sium carbonate, another standard filler [68]. The tin
491 may be a residue from paint tubes made of this material
492 since it was found only in the *Vilhelm Pacht* sample, dat-
493 ing back to before 1909. Moreover, iron was detected by
494 SEM–EDX only in a grain of the *Grumbacher* pre-tested,
495 which might support the abovementioned hypothesis
496 that links this element to contamination.

497 Finally, results obtained by PIXE and SEM–EDX gener-
498 ally agreed, with a few exceptions. The latter technique

499 did not detect certain trace elements (e.g., only zinc was
500 detected in *Vilhelm Pacht*, *Crafint*, and *Grumbacher*
501 1950s paint tubes). In other cases, such as the *Bocour*
502 (Ba, S and Ca, Mg, S in some grains) and *Lefranc & Bour-*
503 *geois* (Ca, S in some grains) tubes, some elements were
504 only detected by SEM–EDX. The spots analyzed through
505 the two techniques may have been locally richer in some
506 compounds (e.g., driers, additives) due to the complexity
507 and inhomogeneity of their formulations.

508 **Particle morphology and size**

509 This section is dedicated to the characterization of mor-
510 phology and size of ZnO particles based on SEM obser-
511 vations. A classification upon Williamson–Hall analysis of
512 HR–XRD data for a selection of samples is also presented.
513 Results for reference materials are presented first, fol-
514 lowed by results on the rest of the corpus.

515 **Reference samples**

516 The two *Brüggemann* reference samples produced by
517 indirect and direct processes presented particles of dis-
518 tinct size and morphology (Fig. 4):

- 519 • ZnO produced by the indirect method had prismo-
520 idal particles with hexagonal bases 40–400 nm wide
521 (width W, in red) and 40–500 nm long (length L, in
522 blue), as schematized in Fig. 4c;
- 523 • ZnO produced by the direct method had mostly
524 acicular particles (i.e., tetrapod-arms grown from a

525 common core), 60–1250 nm wide and 300–5800 nm
526 long, as defined in Fig. 4d.

527 The third reference, the synthesized ZnO nanosmoke,
528 exhibited tetrapod-like morphology, similar to the direct
529 method ZnO, but at the nanoscale (width < 50 nm,
530 length > 100 nm) [49, 69].

531 The impact of the binder on the characterization of
532 ZnO particle morphology and size was investigated for a
533 couple of powders by comparing them *as-is* and ground
534 in linseed oil. As shown in Fig. 5 for *Brüggemann* indirect
535 ZnO powder and the corresponding paint mockup, the
536 size of the particles is comparable.

537 Zinc white samples of the corpus

538 Powders and paint materials mainly showed prismatic
539 morphology (Table 4, Fig. 6a), like the *Brüggemann* indi-
540 rect ZnO powder. However, particles with acicular mor-
541 phology were also observed in some samples, such as the
542 *Vieille Montagne* powders¹² (Fig. 6b) and *Ripolin* and *Tal-*
543 *ens* paint materials.

544 All the samples were quite heterogeneous in size, as
545 shown in Fig. 6c (*Talens* paint tube).

546 An overview of the observations is provided in Table 3;
547 detailed results are in Additional file 2: Table S2.2. Our
548 findings agree with Johnson's observations [9], who noted
549 their consistency with the optimal particle range of 0.2–
550 0.8 μm for paint opacity, durability, and gloss.

551 Since it was not possible to unequivocally classify the
552 samples based on SEM images, in-depth diffraction stud-
553 ies were performed at the synchrotron radiation facil-
554 ity ESRF in Grenoble (France) to estimate the apparent
555 size, aspect ratio, and strain of the ZnO crystallites.
556 The results of the Williamson-Hall analysis are shown
557 in Fig. 7, where the length along the direction (00 l) has
558 been plotted against the length along (hk0). The values
559 were calculated as described in the Additional file 1.

560 Figure 7 shows two clusters of samples, with decreasing
561 sizes for the most recent ones (in blue). *Vieille Montagne*
562 and *Lefranc* samples are all larger than one micrometer.
563 In this cluster is also the *Vilhelm Pacht* tube, which dates
564 back to the end of the 19th/beginning of the 20th cen-
565 tury. Moreover, samples presenting prismatic and acicu-
566 lar morphologies had generally larger crystallites (framed
567 in red in Fig. 7). The smaller particles (< 600 nm) cluster
568 included the most recent *Lefranc & Bourgeois* samples,
569 the *Sennelier* historical powder, and 20th-century sam-
570 ples like the *Maimeri* color chart and paint tube.

571 Results from the Williamson-Hall analysis were gener-
572 ally coherent with SEM observations, but in some cases,
573 the method overestimated¹³ or underestimated¹⁴ the
574 size of some particles compared to SEM. In particular,
575 *Brüggemann* direct ZnO powder and the *Talens* pris-
576 tine paint tube presented larger particles in SEM images
577 than the values estimated by Williamson-Hall analysis
578 (Table 3; Additional file 2: Table S2). This shows the limi-
579 tations of the method, which is unsuitable for assessing
580 the size of crystallites larger than one micrometer and
581 for samples with a broad size distribution. The estimated
582 value is a non-weighted average that may not represent
583 the size distribution. However, the method is still helpful
584 for comparing samples, which is more complex through
585 SEM images. These are high-magnification images of
586 a specific sample area, which might not represent the
587 whole sample. Moreover, it is hard to find a metric based
588 on SEM images to compare samples to each other, espe-
589 cially with such a broad size distribution.

590 The Williamson-Hall analysis was also a valuable tool
591 to classify paint samples where the ZnO particles were
592 difficult to observe using SEM due to the presence of
593 large agglomerates of particles (e.g., the dried yellowed
594 *Talens* tube and the *Lefranc* powder with a binder).

595 By plotting the projection of the average sizes calcu-
596 lated for each peak over the perpendicular planes ab and
597 bc, it was possible to visualize the crystal geometry of the
598 analyzed samples, as shown in Fig. 8.

599 This provides a visual representation of the elongated
600 morphology of ZnO particles (aspect ratio > 1) and of
601 the larger crystallite sizes of historical materials, here
602 represented by *Vieille Montagne* powders and a *Lefranc*
603 1930s paint tube (respectively in green, orange, and red
604 in Fig. 8), compared to modern ones (in light and dark
605 blue and black in Fig. 8). Moreover, the highest aspect
606 ratio values were obtained for the synthesized ZnO
607 nanosmoke (2.1) and *Vieille Montagne* and *Lefranc* sam-
608 ples (2.2–2.8), which might mirror the presence of acicu-
609 lar particles besides prismatic ones.

610 Finally, the calculated strain coefficient was similar for
611 all the analyzed samples (~0.01%), meaning that most
612 differences in peaks broadening are related to size rather
613 than strain effects.

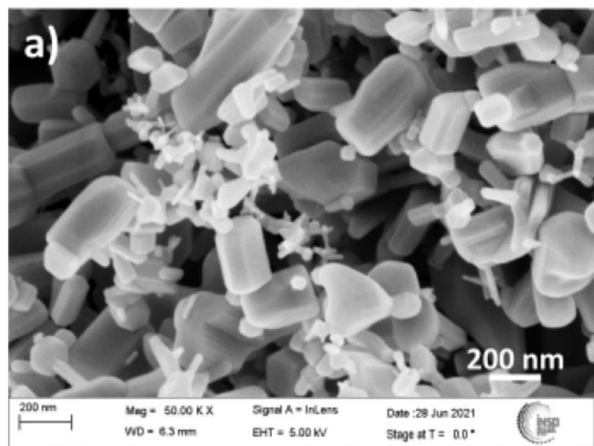
614 A summary of the results of the Williamson-Hall analy-
615 sis is available in Additional file 2: Table S2.3.

12FL01
12FL02 ¹² Except the *Vieille Montagne* “cachet argent” powder, which exhibited only prismatic morphology.

13FL01
13FL02 ¹³ Usually in terms of length for samples like *Fezandie & Sperrle* powder and *Lefranc & Bourgeois* paint tube.

14FL01
14FL02 ¹⁴ Usually in terms of width for samples like *Vieille Montagne* and *Merck* powders.

Indirect Zinc White



Direct Zinc White

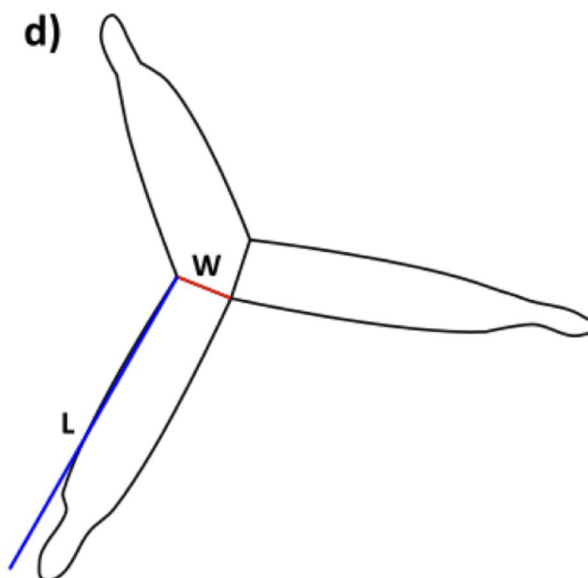
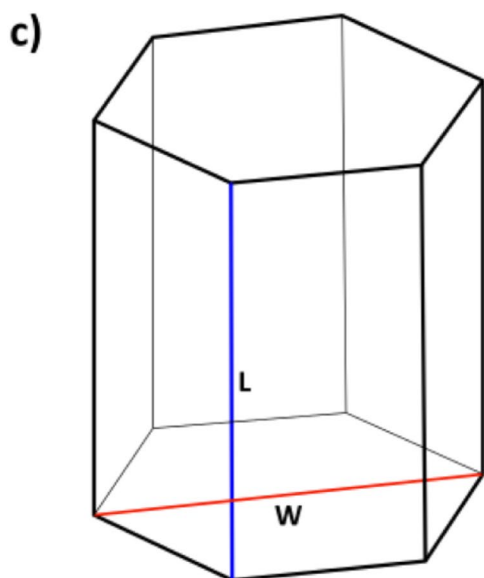
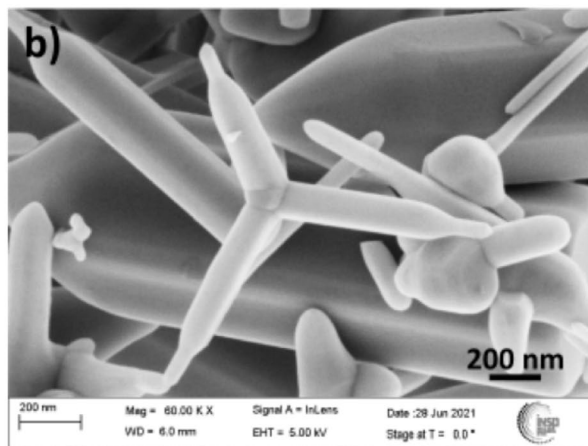


Fig. 4 SEM images (secondary electrons, 5 kV, working distance ~6 mm) of ZnO powders by *Brüggemann* (at the top): **a** indirect method; **b** direct method; schema of the main ZnO morphologies (at the bottom): **c** prismoidal shape of hexagonal basis; **d** acicular shape. The length (L) and width (W) measured on SEM images are also indicated

616 **Luminescence**

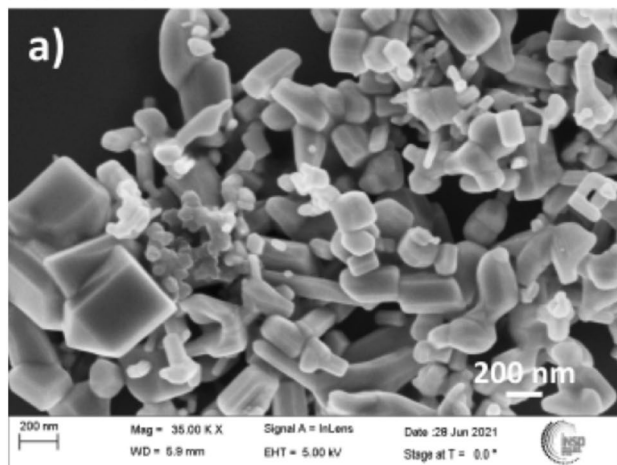
617 This section is dedicated to the luminescence of the analyzed samples. After a short introduction to the luminescence behavior of ZnO, results of the behavior under UV at optical microscopy will be presented, followed by observations at cathodoluminescence. Finally, findings from IBIL will be briefly presented.

623 Luminescence is strictly linked to the electronic structure of ZnO. In the case of perfect crystals, the radiative recombination of excitons generated with excitation energy larger than the energy band gap (EBG) results in emission energy equal to the EBG, the so-called near

band edge (NBE), or fundamental emission. However, when intrinsic or extrinsic defects are present, they create further energy levels within the band gap, available for excitons to recombine. This results in emission energies lower than the EBG. Therefore, the luminescence behavior directly measures crystal quality (i.e., the presence or absence of defects). The fundamental emission of ZnO is at ~3.2 eV (~390 nm); Zhang et al. [49, 69] attributed green photoluminescence (~530–590 nm) to oxygen vacancies, blue/violet photoluminescence (~430 nm) to interstitial zinc (due to synthesis in non-equilibrium conditions and rapid quenching, which favors Zn-rich

628
629
630
631
632
633
634
635
636
637
638
639

Powders



In linseed oil

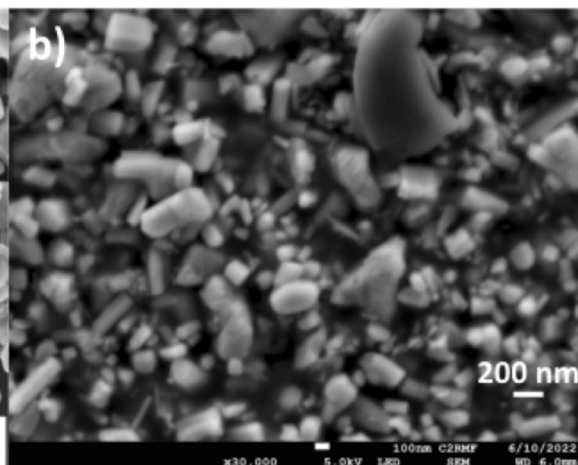


Fig. 5 SEM images (secondary electrons, 5 kV, working distance ~6 mm) of ZnO powder by *Brüggemann*: **a** as-is; **b** ground in linseed oil

640 zinc oxide), and yellow photoluminescence (~600 nm) to
 641 interstitial oxygen-related species.

642 Photoluminescence under UV at the optical microscope

643 The three references presented two types of lumines-
 644 cence, blue or green, as illustrated in Fig. 9. Indirect ZnO
 645 had grains of weak blue luminescence under UV (Fig. 9a,
 646 b). In contrast, direct ZnO had a bright green lumines-
 647 cence (Fig. 9c, d), and ZnO nanosmoke an overall green
 648 (but less bright) luminescence with blue-fluorescing
 649 areas (Fig. 9e, f).

650 The rest of the corpus presented blue, green, blue-
 651 green, or orange luminescence (Fig. 10).

652 All the powders and most paint samples presented
 653 green luminescence under UV, similar to the *Brügge-*
 654 *mann* direct ZnO powders and the synthesized ZnO
 655 nanosmoke. About one-quarter of the paint samples
 656 exhibited blue luminescence similar to the *Brüggemann*
 657 indirect ZnO powders. Four paint samples had green-
 658 blue luminescence. Some samples presented lumines-
 659 cent grains of different colors and intensities, as shown in
 660 Additional file 2: Table S2.4.

661 Three samples, all from the Netherlands and contain-
 662 ing hydrozincite, stood out from the corpus for their
 663 orange luminescence (Fig. 10c, d): these are all but one
 664 *Maastrichtsche* powder¹⁵ (i.e., *Serena Witzegele*, *Roedzegele*
 665 *n°1*, *Grijzegele n°3*). The same luminescence was observed
 666 on the *Sikkens* powder, mainly composed of hydrozincite.

Table 4 Morphology of zinc white samples based on SEM observations

Samples	Morphology	
	Prismatical	Acicular
★ <i>Brüggemann indirect</i> , <i>Fezandie & Sperle</i> , <i>KF Chemicals</i> , <i>Kremer 2010 and 2021</i> , <i>Sennelier</i> , <i>Sennelier</i> , VM “cachet argent”	✔	-
<i>Bocour</i> , <i>Craftint</i> , <i>Grumbacher 1950s</i> , <i>Grumbacher pre-tested</i> , <i>Lefranc & Bourgeois</i> , <i>Maimeri tube</i> , <i>Ripolin</i> , <i>Vilhelm Pacht</i> , <i>Lefranc & Bourgeois tube</i>	✔	✔
★ <i>Brüggemann direct</i> , <i>Merck</i> , VM “cachet bleu, blanc, or, rouge”	✔	✔
<i>Ripolin</i> , <i>Talens</i>	✔	✔
★ <i>ZnO nanosmoke</i>	-	✔

Morphology of zinc white samples. Reference samples are indicated with a star. In blue modern samples, in black historical ones. White background for samples in form of powder, gray for samples in form of paint materials

Finally, bright blue luminescence was observed when ZnO nanosmoke was ground in linseed oil¹⁶ (Fig. 11).

Cathodoluminescence

The analyzed samples were classified based on the observed luminescence color, supported by the collected spectra (Figs. 12, 13). Additional file 2: Table S2.4 contains details about peak position and intensity.

Two types of luminescence were observed:

- Blue luminescence, as for the ZnO produced by the indirect method and the synthesized ZnO nanosmoke (brighter than the previous one), with an

¹⁵ *Maastrichtsche Serena Roedzegele* did contain hydrozincite (detected by XRD and FTIR), but exhibited green luminescence.

¹⁶ The same results were observed when using two types of linseed oil.

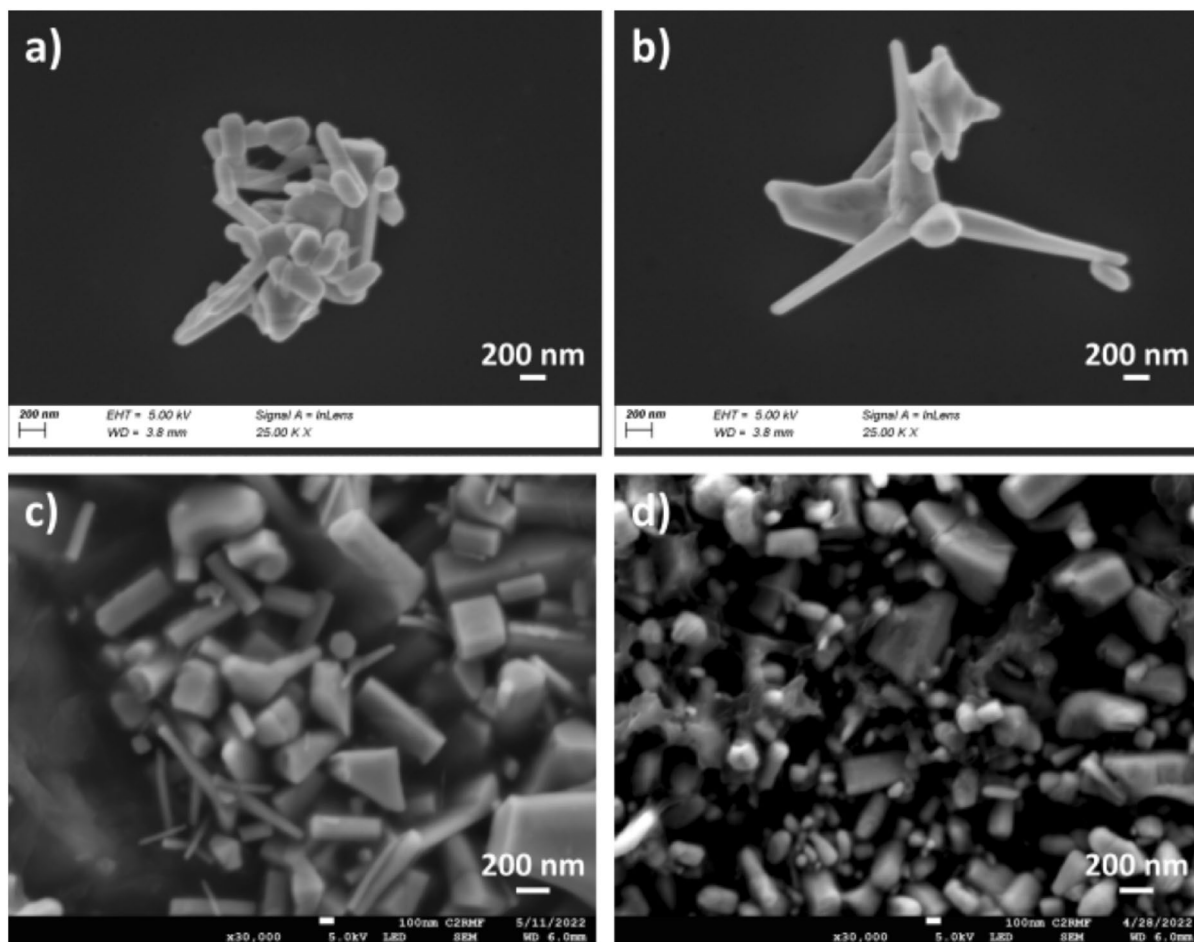


Fig. 6 SEM images (secondary electrons, 5 kV, working distance ~6 mm) of **a–b** *Vieille Montagne* white seal ZnO powder; **c** *Talens* paint tube; **d** *Lefranc & Bourgeois* paint tube

678 intense peak at ~390 nm; the latter also presented a
 679 shoulder at ~430 nm and a larger band at ~530 nm
 680 (Fig. 12a, c);
 681 • Green luminescence for ZnO produced by the
 682 direct method, with a large intense band at ~530 nm
 683 (Fig. 12b).

684 The peak at 390 nm will be indicated as NBE (Near
 685 Band Edge), and the large band at ~530 nm as GL (Green
 686 Luminescence).

687 The results obtained for the entire corpus are described
 688 in Table 5, compared to the luminescence observed
 689 under UV.

690 All the samples in the form of powders exhibited green
 691 luminescence (Fig. 13a) except for *Kremer*, which was
 692 blue-fluorescing. On the other hand, paint tubes were
 693 mostly blue-luminescent (Fig. 13b), except for the green-
 694 luminescent *Lefranc*, *Ripolin*, and *Talens* samples. Blue-
 695 luminescent American paint tubes (i.e., *Grumbacher*,

Permanent Pigments, *Bocour*) and the modern *Lefranc &*
Bourgeois paint tube also had green-fluorescing grains,
 which would explain the appearance of the GL band in
 the corresponding spectra (Fig. 13c).

Green luminescence was generally more intense than
 blue luminescence; thus, exposure conditions had to be
 slightly adjusted for some samples, such as *Vieille Mon-*
tagne, *Sennelier*, direct ZnO powders, and *Talens* and
Craftint paint tubes.

The color of the luminescence observed at cathodolu-
 minescence did not always match that observed at OM
 under UV (Table 5), as in the case of ZnO nanosmoke
 (Fig. 14a, b), the *Talens* paint tube (Fig. 14c, d) and the
 Dutch powders.

Finally, the presence of a binder affected the intensity
 of the peaks but not their position, as shown on mockups
 prepared with *Brüggemann* indirect and direct ZnO and
 linseed oil (Fig. 15).

696
697
698
699
700
701
702
703
704
705
706
707
708
709
710
711
712
713

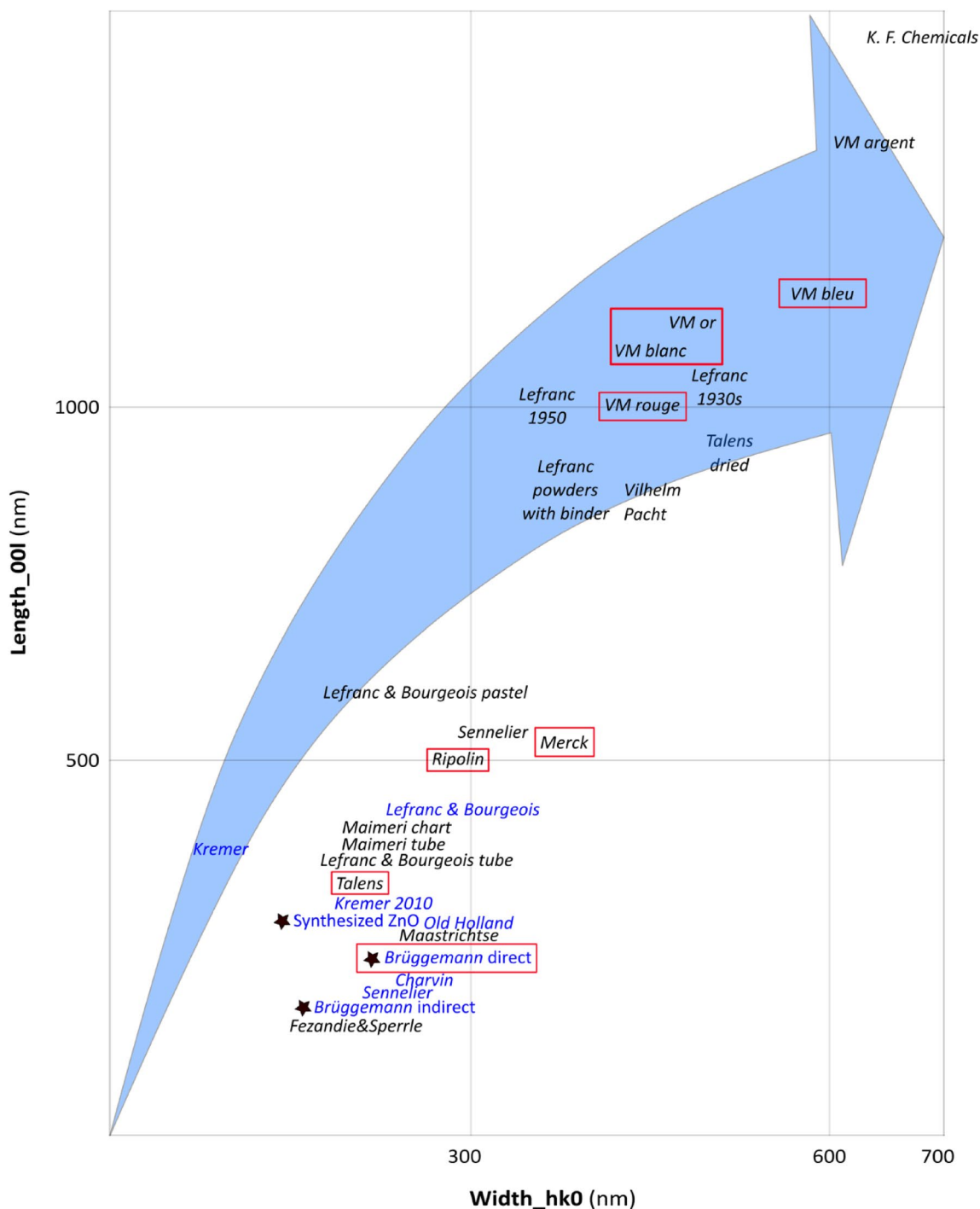


Fig. 7 Size trend of the samples based on results of the Williamson-Hall analysis. Reference samples are indicated with a star. In blue modern samples, in black historical ones. Framed in red are samples also containing acicular particles. Values larger than 1000 nm are not reliable anymore

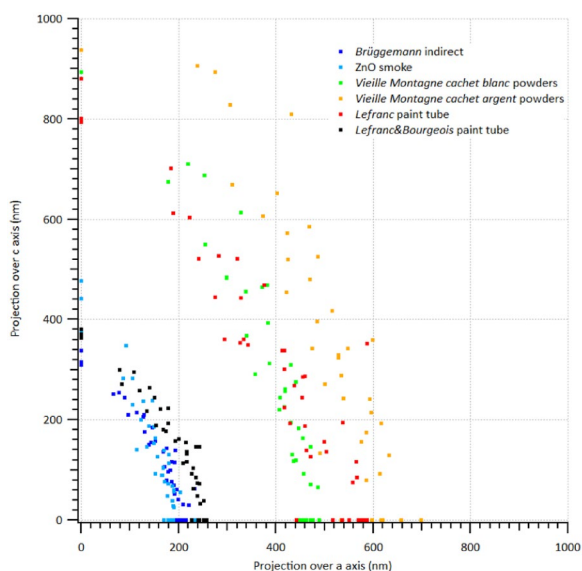


Fig. 8 Representation of the crystal geometry—(a^* , c^*) cross section of ZnO crystallites based on average crystal sizes computed by Williamson–Hall analysis of *Bruggemann* indirect ZnO powder (blue), ZnO nanosmoke powder (light blue), white seal *Vieille Montagne* ZnO powder (green), silver seal *Vieille Montagne* ZnO powder (orange), *Lefranc* 1930s paint tube (red), *Lefranc & Bourgeois* paint tube (black)

714 **Ion beam-induced luminescence**

715 IBIL analyses were also performed on the samples analyzed by PIXE. As for photoluminescence under UV, the general trend of IBIL results did not perfectly agree with CL findings. Additional file 2: Table S2.4 shows details about peak position and intensity.

720 Since the perceived color comes from the ratio of microscopic green and blue-fluorescing particles [9], these differences may arise from diverse sources: imperfect exposure conditions; inhomogeneity of some samples, especially paint tubes¹⁷; different excitation/emission paths¹⁸ induced by the various techniques; damage from high-energy radiation in ionoluminescence.

727 The different excitation/emission paths may be explained by the fact that electrons and protons are massive and carry more momentum than photons; this may lead to different selection rules for cathodo- and ionoluminescence than UV-photoluminescence. The high energy of electrons and protons may generate multiple excitation paths, resulting in relaxation pathways with

17FL01 ¹⁷ For example, the historical *Lefranc & Bourgeois* paint tube also contained Ca, Si, S, and P upon SEM-EDX point analyses. The fact that analyzing just a limited area of complex heterogeneous materials intrinsically presents the risk of not necessarily obtaining representative results.

18FL01 ¹⁸ The width of the GL band varies compared to the NBE, which might suggest the presence of different defects.

734 corresponding cathodo- and ionoluminescence signals different than those detected by photoluminescence. The higher energy of these particles may also lead to a more efficient excitation process, providing additional intermediate states.

739 **Discussion**

740 The discussion of the results is organized into four parts. Insights on colormen practices will be provided first. Then, our findings will be discussed to make a hypothesis on the synthesis process used to manufacture the samples, followed by the relevant trends found in the corpus with a focus on luminescence behavior.

746 **ZnO manufacturers and colormen practices**

747 The variety of brands forming the corpus allowed us to highlight some of their practices.

749 Concerning ZnO manufacturers, the comparison *Vieille Montagne-Maastrichtsche zinkwit Maatschappij* underlines the high purity of powders manufactured by the two companies, especially of the first. Purity is one of the main properties colormen look for in their raw materials. Thus, our findings on *Sennelier* and *Vieille Montagne* powders attested to the continuous high-quality provisioning of the first and the purity of the products provided by the latter.¹⁹

758 However, the complex formulation of some paint tubes like *Sennelier's* and *Maimeri's* (Table 3; Additional file 2: Table S2) confirms the practice of mixing zinc white with other compounds such as barium sulfate [70], lithopone [71], calcium carbonate, zinc sulfide [38] or other pigments like titanium dioxide [72], to modify its optical and mechanical properties or to reduce costs. On the contrary, other paint samples, such as *Lefranc* and *Lefranc & Bourgeois*, did not contain any other compound than ZnO with a binder, coherently with the results of Casadio et al. [48] on an artist-grade *Lefranc* paint tube.

769 However, differences were observed even for the same manufacturer. The dried yellowed *Talens* paint tube presented larger particles than the pristine one. Did ZnO come from different batches of raw materials even though the tubes were sold in the same box?

774 Our results also provided information on possible adulteration due to the mismatch between products' labels and their actual content. This is relevant information to consider for the analysis of artworks and the material history of paint materials.

779 Finally, modern formulations are not synonymous with more transparent labeling, as proved by the presence

19FL01 ¹⁹ *Sennelier* did buy ZnO from the *Vieille Montagne* at least during the first half of the 20th century. Personal communication.

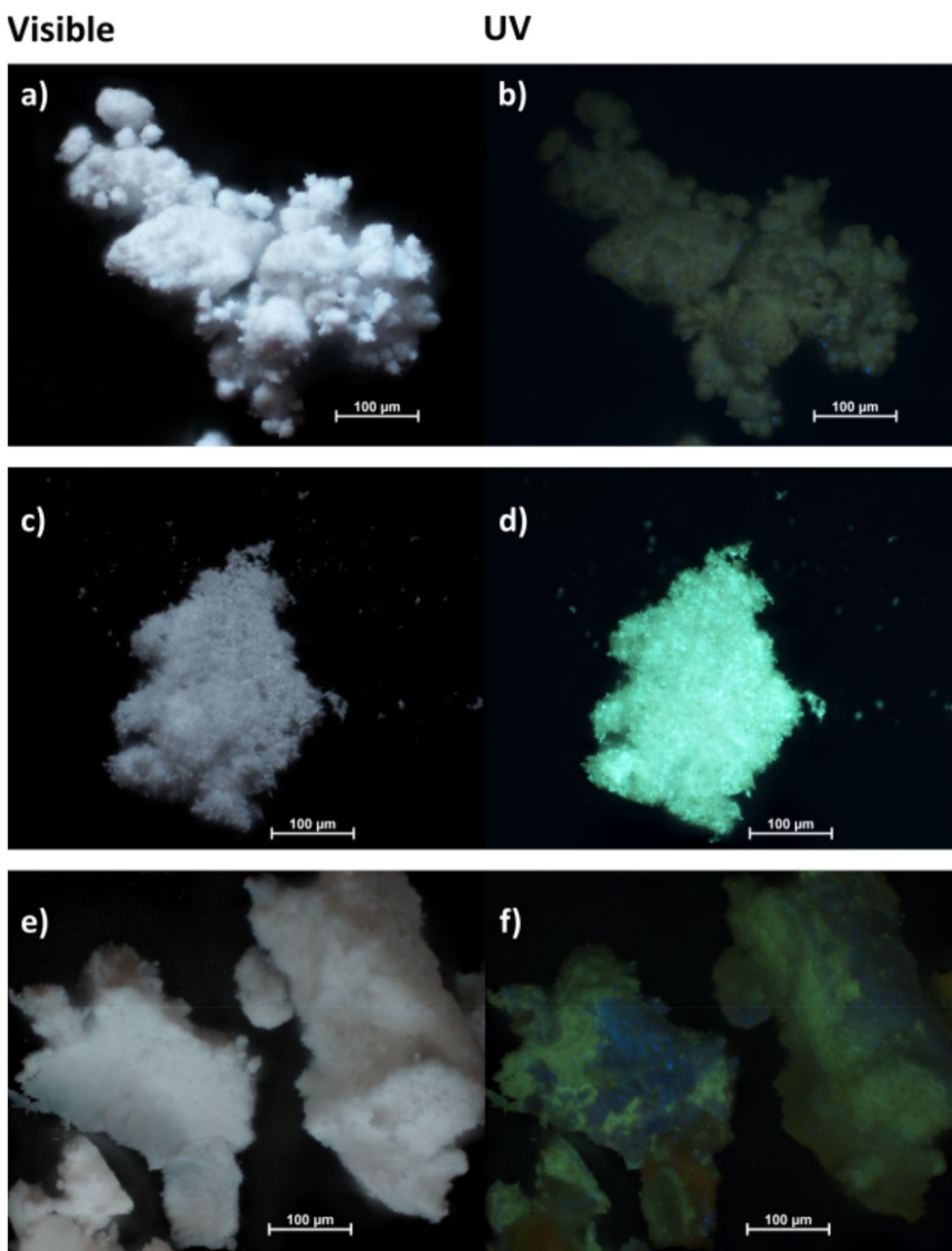


Fig. 9 Images at the OM (20x, under visible light on the left, under UV on the right) of the reference samples: **a–b** *Brüggemann* indirect ZnO; **c–d** *Brüggemann* direct ZnO; **e–f** ZnO nanosmoke

781 of unmentioned additives (10–35 wt%) in modern zinc
 782 white products (e.g., *Old Holland* and *Charvin* paint
 783 tubes).

784 **The hypothesis of the indirect process**

785 The findings for pigment powders matched the high
 786 purity standards for ZnO produced by the indirect
 787 method (i.e., ZnO > 99 wt%) [1]. In the same way, the

ZnO particles of the analyzed powders were similar to
 the ZnO indirect reference in terms of morphology and
 size. These results suggest that all the investigated powder
 materials of the corpus might have been produced
 per indirect method, which is also supported by a historical
 booklet from *La Société Vieille Montagne*, stating that
 the company only made ZnO by indirect method to provide
 their customers with the purest products [73].

788
 789
 790
 791
 792
 793
 794
 795

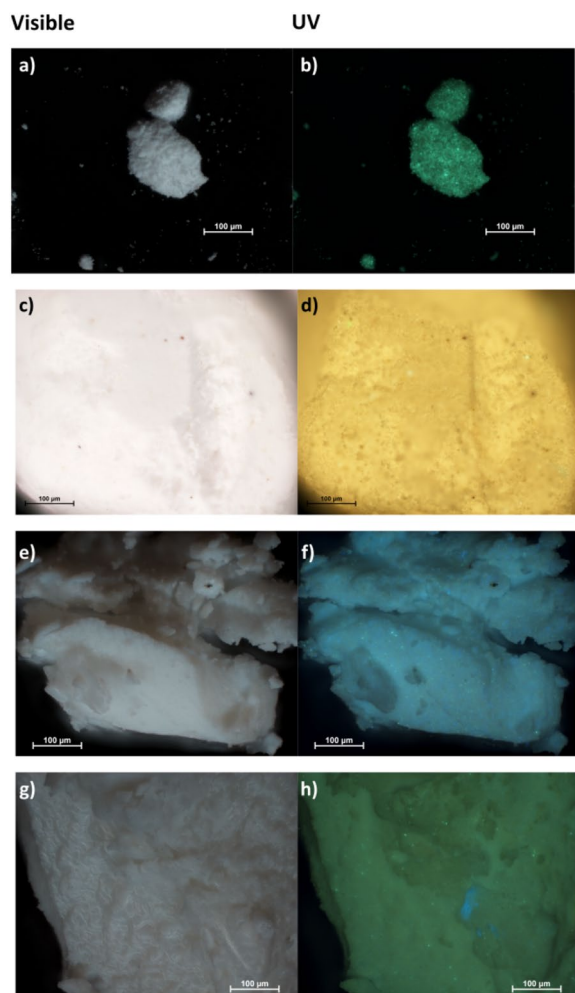


Fig. 10 Images at the OM (20x, under visible light at left and UV at right) of **a–b** *Vieille Montagne* white seal zinc white powder; **c–d** *Maastrichtse zinkwit mij. Ejsden* zinc white powder, “*Roodzegel* n°1”; **e–f** *Lefranc & Bourgeois* zinc white contemporary paint tube; **g–h** *Lefranc* 1930s paint tube

Properties trends

While composition, particle morphology and size, and historical sources pointed out the hypothesis of the indirect process, the observed green photo- and cathodoluminescence (i.e., wide, intense GL band at ~530 nm) of powders and most paint samples were not coherent with the results obtained for *Brüggemann* indirect ZnO (i.e., blue photo- and cathodoluminescence). Already *Artesani et al.* [39] associated samples with both blue- and green photoluminescence to the indirect method, thus to ZnO produced under a Zn vapor-rich environment or in non-equilibrium conditions (i.e., elevated pressure and temperature), for which interstitial zinc is the primary intrinsic defect [39], as found in ZnO nanosmoke [49]. Relying only on the NBE peak to identify zinc white may thus be misleading in some cases. The luminescence behavior will be discussed further in the next paragraph.

The second trend identified in the corpus consists of the smaller size of ZnO particles for the most recent samples. Results on *Vieille Montagne* materials support this hypothesis: while powders produced in the laboratory presented prismatic submicrometer particles, the ones made at the *Valentin-Cocq* site had both prismatic and acicular particles larger than one µm. Less controlled large-scale synthesis conditions may thus have affected their size. This means older samples produced via the indirect method might have larger particles and more defective structures because of poorly controlled synthesis conditions (i.e., growth time, temperature, and atmosphere). This would explain the corpus’ significant size distribution, varied morphology, and luminescence behavior. Similar remarks were also reported by, for example, *Hageraats et al.* [25] and *Capogrosso et al.* [18] in some *Lefranc* samples.

As *Zhang et al.* [49, 69] showed, synthesis conditions are crucial in determining ZnO color and properties. The

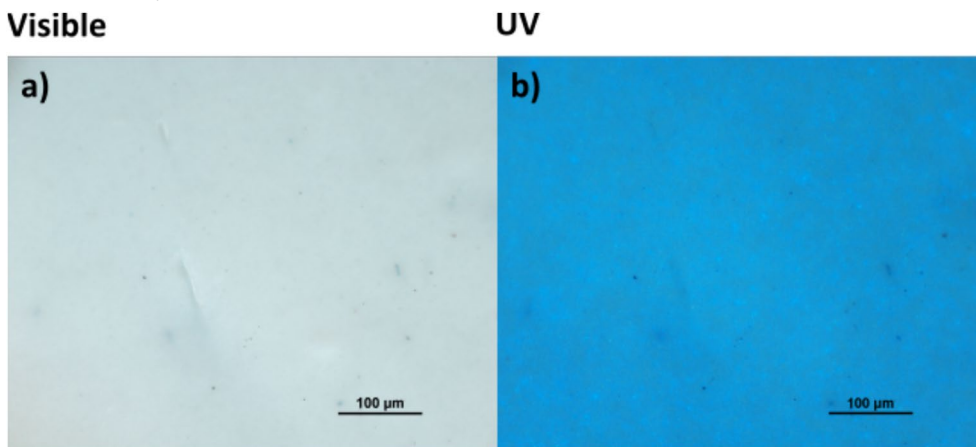


Fig. 11 Images at the OM (20x) of a paint mockup prepared with ZnO nanosmoke and linseed oil under **a** visible and **b** UV light

796
797
798
799
800
801
802
803
804
805
806
807
808
809
810
811
812
813
814
815
816
817
818
819
820
821
822
823
824
825
826
827
828
829
830
831

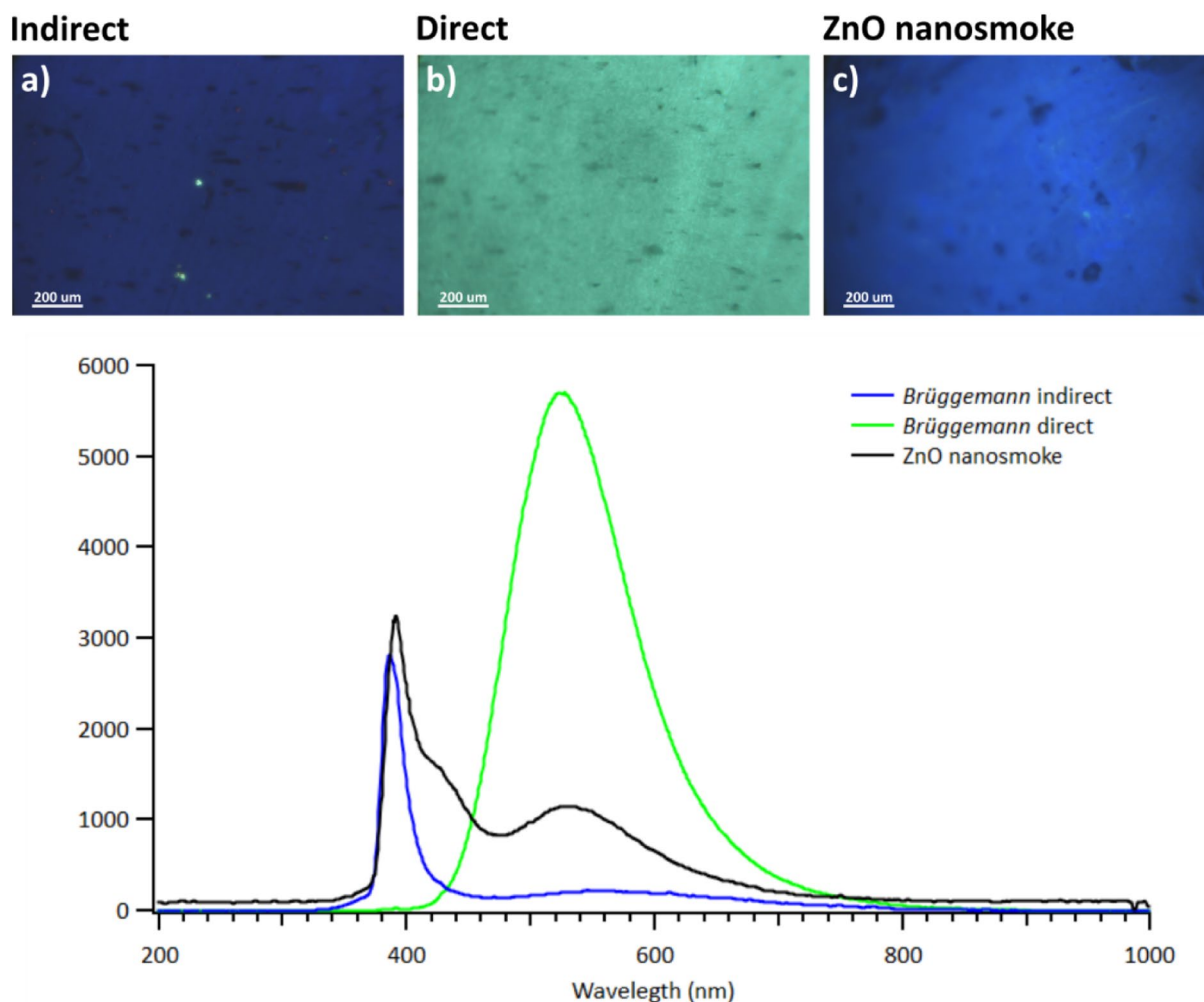


Fig. 12 Cathodoluminescence images (10x, ~390 μA, 11 kV; at the top) of: **a** *Bruggemann* indirect ZnO; **b** *Bruggemann* direct ZnO; **c** ZnO nanosmoke powders. The corresponding spectra are shown at the bottom of the Figure

832 tetrapod-like ZnO nanosmoke used as a reference in this
 833 study can acquire hexagonal prism morphology if synthe-
 834 sized in an oxygen-rich atmosphere [69], the morphol-
 835 ogy most observed in the corpus. They also showed that
 836 Chemical Vapor Synthesis (i.e., dynamic conditions under
 837 gas flow, controlled temperature, and pressure) leads to
 838 smaller, more homogeneous particles (length < 50 nm)
 839 [69]. This might prove the link of morphology and size of
 840 ZnO nanoparticles to oxygen pressure during synthesis
 841 or, more generally, to the control of synthesis conditions,
 842 which may have improved over time, leading to smaller
 843 particles of narrower size distribution.

844 A third trend concerns trace elements, possibly help-
 845 ful in distinguishing historical from modern ZnO, at
 846 least for samples in the form of powders. While historical
 847 samples (e.g., *Vieille Montagne*, Dutch powders) consist-
 848 ently contained traces of lead and sulfur, modern ones
 849 included other elements like calcium and chlorine. This

could be related to the fact that historical zinc white was
 likely produced using the same raw materials (i.e., zinc
 ores). In contrast, modern zinc white has a more complex
 supply chain, employing minerals from other parts of the
 world or recycled zinc, which could be contaminated.

Luminescence of zinc white

As mentioned above, luminescence was not directly cor-
 related to other features of zinc white. Two hypotheses
 are presented here to describe the observed trends and
 their connection to other zinc white properties.

The NBE emission predominant in defect-free ZnO
 crystals was almost undetectable in some zinc white sam-
 ples (i.e., *Vieille Montagne*, *Fezandie & Sperrle*, *Merck*
 powders; *Lefranc*, *Talens*, *Vilhelm Pacht* paint tubes).
 These were primarily historical materials with larger ZnO
 particles (Fig. 16), a trend already observed by Clementi
 et al. [36] in paint mockups.

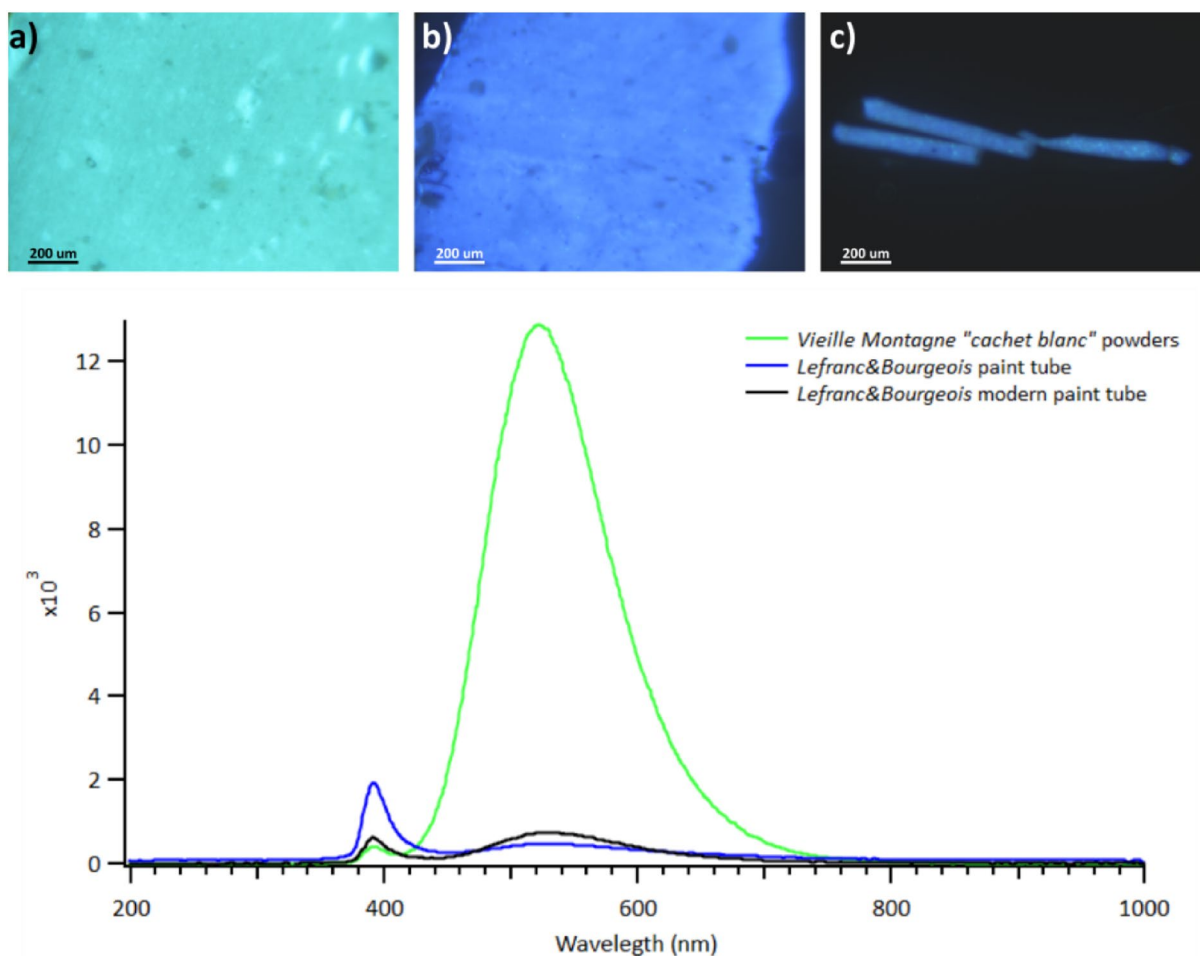


Fig. 13 Cathodoluminescence images (10x, ~390 μA, 11 kV; at the top) of **a** *Vieille Montagne* white seal zinc white powders; **b** *Lefranc & Bourgeois* zinc white paint tube; **c** *Lefranc & Bourgeois* modern zinc white paint tube. The corresponding spectra are shown at the bottom of the Figure

867 Therefore, a first proposition correlates the GL to
 868 larger ZnO particles. Samples with larger particles and
 869 GL might once have had a less intense GL band, typical
 870 of the indirect method, and turned green-luminescent
 871 over time. Johnson [9] demonstrated that blue-fluorescing
 872 particles can shift to green-fluorescing particles over
 873 time via oxygen removal. Moreover, the role of oxygen
 874 on the luminescence behavior of ZnO was already high-
 875 lighted by Morley-Smith [37], who observed a relation
 876 between the GL and the ZnO particle size and related it
 877 to the oxygen at the surface of ZnO particles.

878 Zhang et al. [69] recently showed that the GL band
 879 indicates a more defective material rich in oxygen vacan-
 880 cies. However, they attributed their presence to the oxy-
 881 gen pressure conditions used in the synthesis rather than
 882 to the size and morphology of ZnO particles. This leads
 883 to a second hypothesis: historical indirect ZnO with
 884 larger particles may exhibit more intense GL after manu-
 885 facturing due to less controlled synthesis conditions.

The ratio of blue-to-green-fluorescing particles has
 been correlated to the photo-activity of ZnO, being
 higher for blue-fluorescing particles (e.g., higher chal-
 king²⁰ rates observed for house paint) [9, 37], preva-
 lent type in ZnO produced via the indirect method. To
 solve the issue, back in the 1950s, *Durham Chemicals*
 developed a ZnO indirect grade of larger green-lumi-
 nescent particles (i.e., lower oil absorption and reactiv-
 ity, higher reducing power) that could resist chalking
 [20], which proves the existence of different types of
 indirect ZnO. Hageraats et al. [74] also observed differ-
 ent types of zinc white in painting materials. This infor-
 mation is particularly relevant in light of the results of
 Hermans et al. [35], for example, who showed that zinc
 whites of different reactivity can be observed in paint-
 ings and potentially affect paint performance, especially

886
887
888
889
890
891
892
893
894
895
896
897
898
899
900
901

²⁰ A result of the oxidation of the binder due to peroxides formation.

Table 5 Comparison of photoluminescence under UV and cathodoluminescence of zinc white samples

Samples	Under UV	CL
★ <i>Brüggemann indirect</i>	Blue	Blue
<i>Lefranc & Bourgeois tube, Bocour Titan-zinc white</i>		
<i>Blockx, Maimeri color chart, Old Holland, ZnO nanosmoke mockups</i>		Not performed
<u><i>Kremer 2010 and 2021, ★ ZnO nanosmoke</i></u>	Green	Blue
<i>Lefranc & Bourgeois, Maimeri paint tube, Craftint, Grumbacher, Permanent Pigments watercolor</i>		
★ <i>Brüggemann direct, Fezandie & Sperrle, KF Chemicals, Merck, Sennelier, VM cachet or, argent, blanc, rouge et bleu</i>		Green
<i>Ripolin, Talens</i>		
<u><i>Maastrichtse Serena roodzieaël</i></u>		Not performed
<i>Blockx^a, Charvin, Grumbacher, Lefranc 1950, Lefranc powders with a binder, Lefranc & Bourgeois pastel, Michael Harding, Ripolin, Sennelier acrylics</i>	Blue-green	Blue
<i>Vilhelm Pacht, Bocour, Talens dried</i>		Green
<i>Lefranc 1930s</i>		
<u><i>Maastrichtse Serena Grizzeael n°3, Roodzeael n°1, witzeael</i></u>	Orange ^b	Blue-green

Color of the luminescence under UV and at cathodoluminescence. Reference samples are indicated with a star. In blue modern samples, in black historical samples. Samples containing hydrozincite are underlined. White background for samples in form of powder, gray for samples in form of paint

^a Zinc white and titan-zinc white

^b The *Sikkens* powder made of hydrozincite also exhibited orange luminescence under UV light and blue luminescence at CL

(Table 5). Hydrozincite might affect the photoluminescence of zinc white only when present above a specific concentration since other ZnO samples containing some hydrozincite presented green luminescence (e.g., *Maastrichtse Serena Roedzeegel* powder). However, the contribution of other compounds to the photoluminescence response of these samples cannot be excluded either. Further studies on these materials and hydrozincite will be performed to confirm these preliminary hypotheses on the orange photoluminescence.

Finally, optical cathodoluminescence, a technique widely used in geology [76], more rarely to study paint materials [77–79], proved an appropriate, easy-to-handle tool for identifying zinc white vs. other whites and zinc-based pigments. Our results add up to the research of Palamara et al. [77], the only systematic study of white pigments by cathodoluminescence presented until now, to the authors’ knowledge. They showed applications of SEM-CL aimed at building a database of the behavior of pigments at cathodoluminescence. In a complementary way, our study demonstrates a more accessible method to assess chemical differences through visual information (i.e., a large field image at the OM) and spectral features (spectroscopy). Once further reference databases are developed, the method could be of great value, especially in distinguishing zinc white from other zinc-based pigments (e.g., lithopone, cobalt green, and zinc yellow).

Conclusions

The study of a unique, varied corpus of historical and modern zinc white artists’ materials provided information on the variability of the properties of the pigment and colormen practices for zinc white formulations. The corpus presented some unavoidable biases and intrinsic limitations but still represents a good reference of zinc white properties for Heritage professionals.

Common additives, proportions, and combinations were identified for various color manufacturers and compared to their labeling, providing information about zinc white materials, their properties, and possible manufacturers’ and artists’ choices.

Hydrozincite was detected in some ZnO powders, even as the main component in the *Sikkens* powder; it was not found in any paint sample. The compound is likely a degradation product formed over time in powders exposed to air. It was identified by XRD and FTIR, which have different sensibilities to the compound but provide coherent results. In our corpus, the presence of hydrozincite had no impact on the cathodoluminescence response of ZnO samples, but it might be a cause of the orange luminescence observed under UV. Further studies are required to confirm if hydrozincite or other compounds

in certain environmental conditions, such as upon use of solvents for conservation treatments, which are a trigger for the crystallization of zinc soaps. Moreover, most documented cases of severe degradation due to zinc white involve 20th-century rather than 19th-century artworks [23, 27, 75]; however, this may not be representative of the use and degradation of zinc white, since the pigment may have been employed more extensively from the end of the 19th century.

Nevertheless, it is essential to consider other factors, such as pigment-binder interaction, aging, and the presence of other compounds. In our corpus, barium sulfate—either alone (e.g., *Bocour* paint tube) or with calcium carbonate and zinc sulfide (e.g., *Maimeri* paint tube)—did not modify the cathodoluminescence response of ZnO samples. Hydrozincite did not seem to affect color and spectral features observed at cathodoluminescence either (e.g., in *Kremer* powders, which both presented bluish CL with no other spectral characteristics). Still, it might have played a role in the orange luminescence observed at the OM under UV light for some Dutch powders since all the samples exhibiting an orange luminescence under UV contained this compound

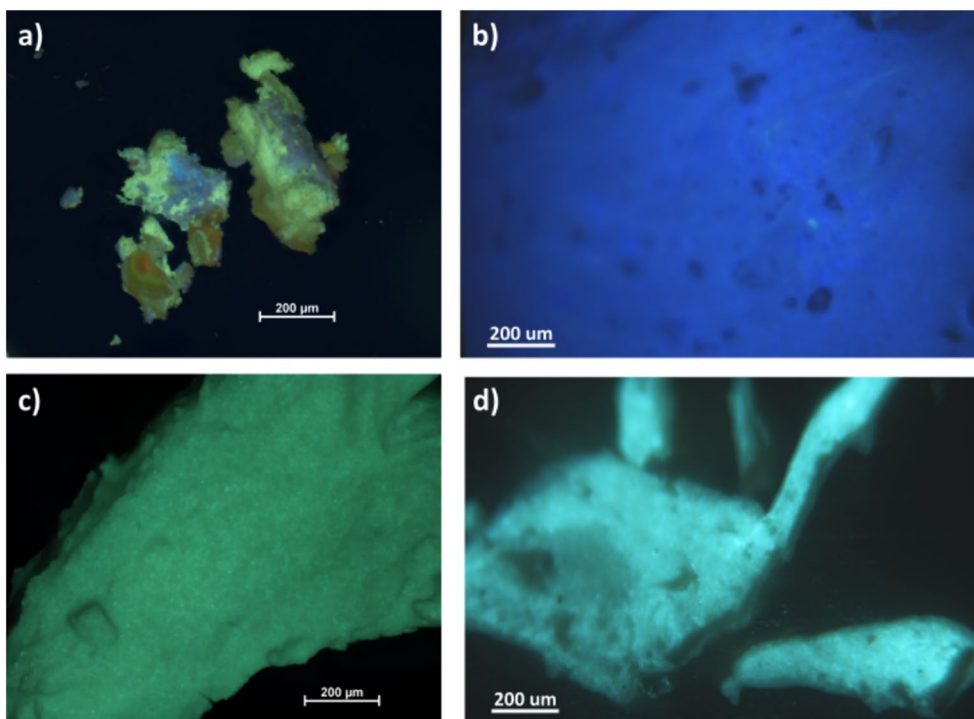


Fig. 14 Images at the OM (10x) under UV (on the left) and at cathodoluminescence (on the right) of **a, b** ZnO nanosmoke powders; **c, d** Talens paint tube

976 are responsible for this behavior. Since crystallographic
 977 research on hydrozincite has not been published since
 978 the 1960s, the compound will be the object of another
 979 study.

980 The results for indirect and direct ZnO references
 981 agreed with the literature. The samples' high purity (i.e.,
 982 a reduced amount and type of trace elements), prismo-
 983 idal morphology, and submicron particle size match the
 984 characteristics of the ZnO synthesized via the indirect
 985 method. Acicular particles were sometimes observed in
 986 historical samples in addition to prismatic ones, with a
 987 large particle size distribution for the whole corpus.

988 The luminescence behavior was indeed not straight-
 989 forward to interpret. Both blue- and green-fluorescent
 990 materials were observed. The Near-Band-Edge peak
 991 at ~390 nm was not always detectable, even in pure
 992 historical powders without binders. This raises ques-
 993 tions on the practical use of this feature for identifying
 994 zinc white. We formulated two hypotheses to explain
 995 that either blue-luminescent particles might have turned
 996 green-luminescent over time or some (less controlled)
 997 synthesis conditions promoted the formation of larger
 998 green-luminescent particles.

999 Modern materials had smaller ZnO particles than
 1000 historical ones, containing some recurring trace elements,
 1001 such as lead and sulfur.

1002 Photo-, cathodo- and ionoluminescence results did not
 1003 perfectly match. Cathodoluminescence proved a valu-
 1004 able complementary tool for studying pigments and paint
 1005 materials. To the authors' knowledge, this technique,
 1006 combined with optical microscopy, was used for the first
 1007 time on such a large corpus of paint materials. Photolu-
 1008 minescence seems more sensitive than cathodolumines-
 1009 cence to the presence of compounds other than ZnO
 1010 (e.g., probably hydrozincite), so comparing the two tech-
 1011 niques can be informative of compositional variations of
 1012 the sample.

1013 This study represents a solid database in which syn-
 1014 thesis routes, intrinsic properties, and luminescence
 1015 behavior of zinc white were discussed as a guideline for
 1016 identifying and classifying zinc white. The presented
 1017 findings will be used as a reference to study samples and
 1018 cross-sections from 19th–20th century paintings to sur-
 1019 vey the extent and modalities of the use of zinc white, its
 1020 properties, and its relation to painting degradation.

1021 Archival and historical research on zinc white, its pro-
 1022 duction, and use among 19th and 20th centuries color-
 1023 makers, merchants, and artists will be deepened in an art
 1024 historical review [80].

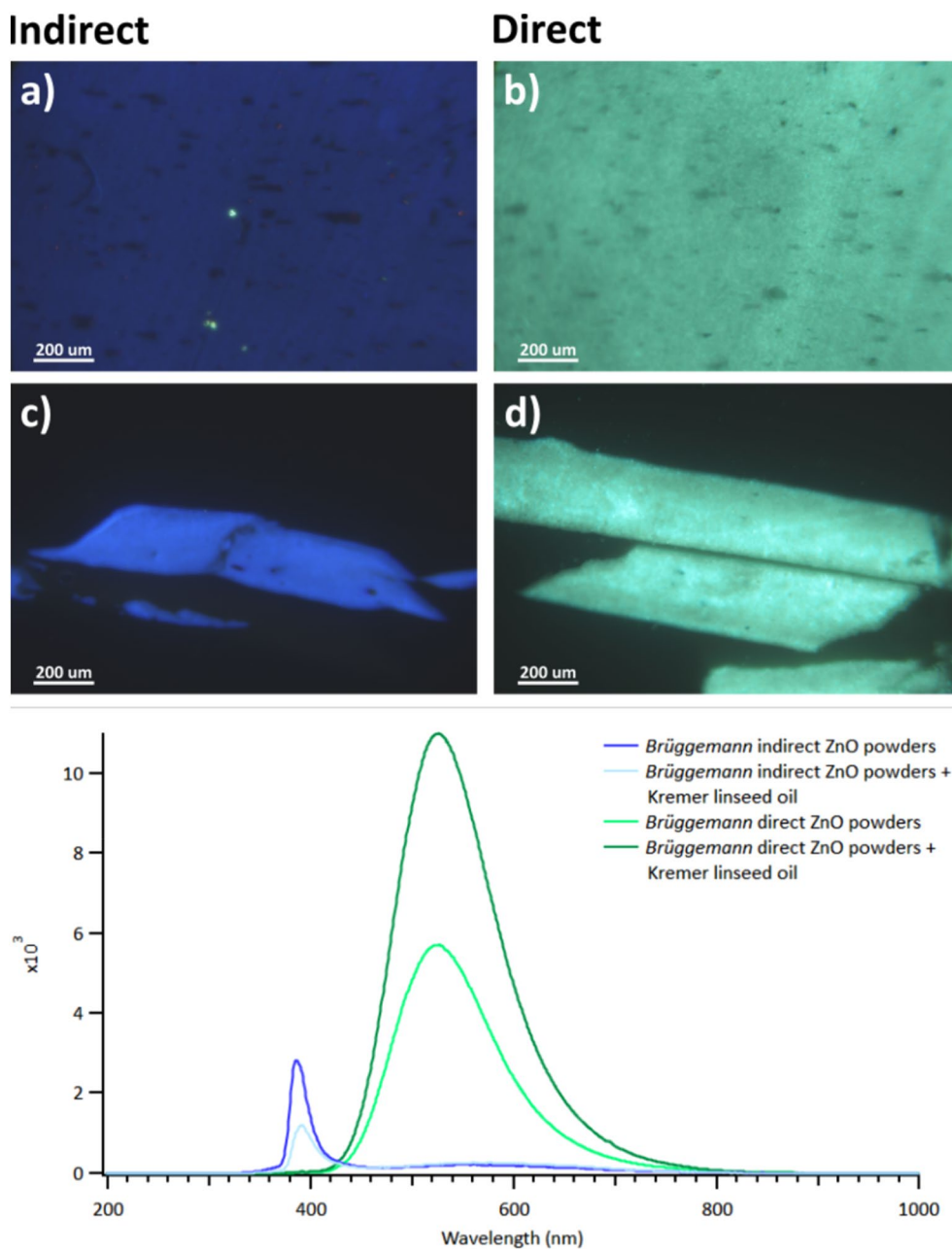


Fig. 15 Cathodoluminescence images (10x) and spectra of *Bruggemann* of **a** indirect ZnO powder; **b** direct ZnO powder; **c** indirect ZnO powder ground in linseed oil; **d** direct ZnO powder ground in linseed oil

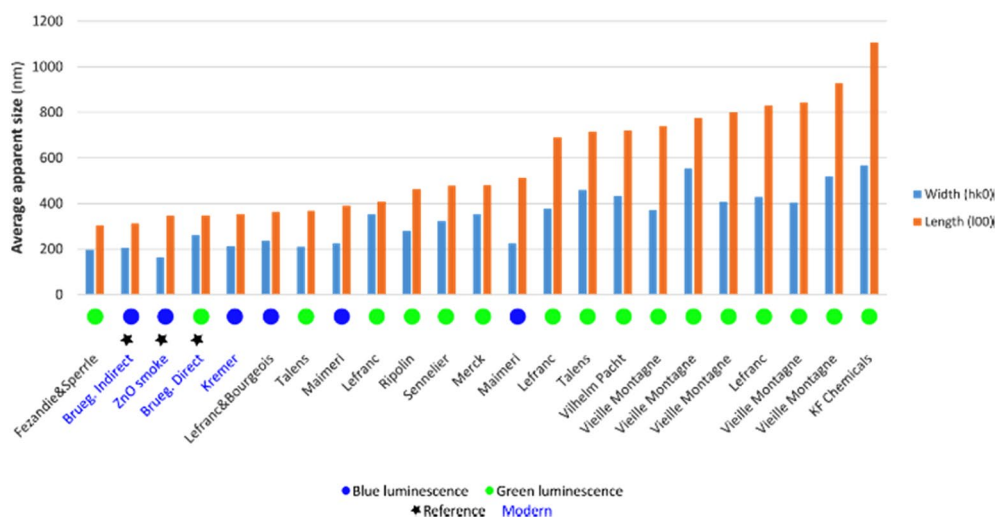


Fig. 16 Size trend of samples analyzed at the ESRF (Williamson-Hall analysis) classified by growing size along the (100) direction (in orange). In comparison, the direction (hk0) is also shown (in blue). With a star are indicated reference samples, in blue are modern samples, and in black are historical ones. Green and blue dots indicate the color observed using cathodoluminescence

1026 Abbreviations

- 1027 CL Cathodoluminescence
- 1028 C2RMF Centre de Recherche et Restauration des Musées de France
- 1029 EBG Energy Band Gap
- 1030 ESRF European Synchrotron Radiation Facility
- 1031 GL Green Luminescence
- 1032 HR-XRD High angular Resolution-X-Ray Diffraction
- 1033 IBIL Ion Beam-Induced luminescence
- 1034 INSP Institut de NanoSciences de Paris
- 1035 IPANEMA Laboratoire Institut Photonique d'Analyse Non-destructive Européen des Matériaux Anciens
- 1036 OM Optical Microscopy
- 1037 NBE Near Band Edge
- 1038 PIXE Particle-Induced X-ray Emission spectroscopy
- 1039 PL Photoluminescence
- 1041 RCE Rijksdienst voor het Cultureel Erfgoed (Cultural Heritage Agency of the Netherlands)
- 1042 SEM-EDX Scanning Electron Microscopy-Energy Dispersive X-ray spectroscopy
- 1044 WH Williamson-Hall
- 1046 XRD X-Ray Diffraction
- 1047 XRF X-Ray Fluorescence spectroscopy

1048 Supplementary Information

1049 The online version contains supplementary material available at <https://doi.org/10.1186/s40494-023-01082-4>.

1051 **Additional file 1: Table S1.** Samples description. **Figure S1.** FTIR spectrum of Sikkens powders. PIXE fitting and Williamson-Hall analysis procedures.

1054 **Additional file 2: Table S2.** Summary of the performed analysis.

1055 Acknowledgements

1056 This work benefited from State aid managed by the *Agence Nationale de la Recherche* (French National Research Agency) under the future investment programme integrated into France 2030, bearing the reference ANR-17-EURE-0021—*Ecole Universitaire de Recherche Paris Seine*—Foundation for Cultural Heritage Sciences. Financial support from the Access to Research Infrastructures activity in the Horizon 2020 Programme of the EU (IPERION HS Grant Agreement n.871034) is gratefully acknowledged. We thank Dr. Ineke Joosten,

Prof. Klaas Jan van den Berg, and Rika Pause for their support during the ARCHLab access at the RCE. Samples from *Maastrichtse zinkwit Maatschappij* and *Sikkens* were kindly provided through this access. We kindly acknowledge all the people and institutions that supported the presented study by providing some samples for building the *corpus* of analysis: *L. Brüggemann GmbH & Co. KG*, Salzstraße 131, 74076 Heilbronn, Germany (Mr. Markus Piotrowsky); *Maison de la Métallurgie et de l'Industrie de Liège*, Boulevard Raymond Poincaré 17, 4020 Liège (Ms. Elena Marcos Alvarez); Sidney and Lois Eskenazi Museum of Art at Indiana University (Ms. Julie Ribits); our colleagues Mr. Gilles Bastian and Ms. Nathalie Balcar from the C2RMF; the Art Materials Research and Study Center at the National Gallery of Art, Washington, D.C. 20565 (Ms. Tammy Hong and Ms. Kimberly Schenck); *Den Hirschsprungske Samling* and the Royal Danish Academy, Copenhagen, Denmark (Prof. Mikkel Scharff and Prof. Cecil Krarup Andersen); *Fondazione Maimeri* (Mr. Sandro Baroni and Ms. Maite Rossi); *Politecnico di Milano* (Prof. Daniela Comelli). The EQUIPEX NEW AGLAE research program (n. ANR-10-EQPX-22, French Ministry of Research) is acknowledged. This work was also carried out in the frame of the NewAGLAE project. We kindly acknowledge Ms. Maëva L'Héronde for her support with SEM images of ZnO powders at IPANEMA and Ms. Dominique Demaille for the SEM images of the reference ZnO powders at the INSP. We acknowledge the European Synchrotron Radiation Facility (ESRF) for providing synchrotron radiation facilities. We thank Dr. Catherine Dejoie for assistance and support using beamline ID22 and Dr. Marine Cotte, Dr. Victor Gonzalez, Dr. Letizia Monico, and Dr. Frederik Vanmeert for the BAG access. We thank the *Laboratoire d'Océanologie et de Géosciences* of the University of Lille for kindly allowing us to use their optical cathodoluminescence system for some samples of the corpus of study. We kindly acknowledge Prof. Didier Gourier and Dr. Thomas Calligaro for taking some time to discuss the luminescence of zinc white and Dr. Elyse Canosa for proofreading the English of the paper. Finally, we thank the reviewers for taking some of their precious time to read and provide their feedback on our work.

Author contributions

JS and NP conceptualized the study. NP and MO carried out SEM analysis. MO carried out OM and FTIR analysis and acquired CL spectra. NP acquired CL images. YC performed, supervised, and supported CL analysis. NP acquired PIXE/IBIL data, supported by QL and LP, for analysis and data treatment. NP acquired HR-XRD data. GW supported and supervised the treatment of HR-XRD data. SS and NP carried out the synthesis of ZnO nanoparticles. NP treated the data and prepared figures and tables. NP wrote the manuscript with the support of JS. MO participated in the writing of the draft. JS supervised the experimental work, contributed to the writing of the paper, and reviewed the manuscript in detail. VE provided advice on the general structure

1105 of the paper and reviewed the manuscript. GW, YC, SS, QL, and LP revised the
1106 paper, focusing on the parts related to their specific areas of expertise. NP,
1107 JS, YC, and SS worked on the review of the paper. All authors have read and
1108 agreed to the published version of the manuscript.

1109 Funding

1110 This work benefited from State aid managed by the *Agence Nationale de la*
1111 *Recherche* (French National Research Agency) under the future investment
1112 program integrated into France 2030, bearing the reference ANR-17-EURE-
1113 0021—*Ecole Universitaire de Recherche Paris Seine*—Foundation for Cultural
1114 Heritage Sciences. Financial support by the Access to Research Infrastructures
1115 activity in the Horizon 2020 Programme of the EU (IPERION HS Grant Agree-
1116 ment n.871034) is gratefully acknowledged for the ARCHLab access at the RCE
1117 in Amsterdam.

1118 Availability of data and materials

1119 The datasets supporting the conclusions of this article are included within the
1120 article and in the Supplementary Materials.

1121 Declarations

1122 Competing interests

1123 The authors declare no competing interests.
1124

1125 Received: 31 March 2023 Accepted: 6 November 2023

1126 References

- 1127 1. Kuhn H. Zinc white. In: Feller RL, editor. *Artists' pigments - a handbook of*
1128 *their history and characteristics*. London: National Gallery of Art, Washing-
1129 *ton Archetype Publications; 1986. p. 169–86.*
1130 2. Gardner HA. *Paint researches and their practical application*. Washington:
1131 *Press of Judd & Detweiler, Incorporated; 1917.*
1132 3. Osmond G. Zinc white: a review of zinc oxide pigment proper-
1133 *ties and implications for stability in oil-based paintings*. *AICCM Bull.*
1134 *2012;33(1):20–9.*
1135 4. Moezzi A, McDonagh AM, Cortie MB. Zinc oxide particles: synthesis,
1136 *properties and applications*. *Chem Eng J.* 2012;185–186:1–22.
1137 5. Amir M, Abbas M, Fatima M, Khan ZS, Shah NA. Synthesis of carbon
1138 *nanotubes and ZnO nanocomposites for IR sensing*. *Appl Phys A.*
1139 *2021;127(11):882.*
1140 6. Zuliani A, Bandelli D, Chelazzi D, Giorgi R, Baglioni P. Environmentally
1141 *friendly ZnO/Castor oil polyurethane composites for the gas-phase*
1142 *adsorption of acetic acid*. *J Colloid Interface Sci.* 2022;614:451–9.
1143 7. Flora RMN, Palani S, Sharmila J, Chamundeeswari M. Green synthesis
1144 *and optimization of zinc oxide quantum dots using the Box-Behnken*
1145 *design, with anticancer activity against the MCF-7 cell line*. *Appl Phys A.*
1146 *2022;128(4):359.*
1147 8. Tyagi N, Ashraf W, Mittal H, Fatima T, Khanuja M, Singh MK. A facile
1148 *synthesis of ternary hybrid nanocomposite of WS₂/ZnO/PPy: An efficient*
1149 *photocatalyst for the degradation of chromium hexavalent*. *Dyes Pigm.*
1150 *2023;210:110998.*
1151 9. Johnson VM. *Ultraviolet-induced fluorescence and photo-degradation*
1152 *in zinc oxide watercolour paints*. Doctoral thesis, Northumbria University.
1153 2020.
1154 10. Rogala D, Lake S, Maines C, Mecklenburg M. Condition problems related
1155 *to zinc oxide underlayers: examination of selected abstract expressionist*
1156 *paintings from the collection of the Hirshhorn Museum and Sculpture*
1157 *Garden, Smithsonian Institution*. *J Am Inst Conserv.* 2010;49(2):96–113.
1158 11. Robb M. *Ivan Le Lorraine Albright paints a picture*. New York: *ArtNews;*
1159 1950.
1160 12. van Driel BA, van den Berg KJ, Gerretzen J, Dik J. The white of the 20th
1161 *century: an explorative survey into Dutch modern art collections*. *Herit*
1162 *Sci.* 2018;6(1):16.
1163 13. Perego F. *Blanc de zinc (Zinc white) Le dictionnaire des matériaux du*
1164 *peintre (The painter's materials dictionary)*. Paris: Belin; 2005. p. 102–7.

- 1165 14. Lefort MJ. *Chimie des couleurs (Colors chemistry)*. Paris: French. V. Mas-
1166 *son; 1855.* 1167
1168 15. Clarke M. A Nineteenth-Century Colourman's terminology. *Stud Conserv.*
1169 *2009;54(3):160–9.* 1170
1171 16. Spennemann DHR. Stanislas Sorel's zinc-based paints. *Trans IMF.*
1172 *2020;98(1):8–13.* 1173
1174 17. de Saint-Paul SG. Société Anonyme des mines et fonderies de zinc de
1175 *la Vieille Montagne, 19 rue Richer Paris (Limited liability company Vieille*
1176 *Montagne - zinc miners and smelters), commercial catalog*. Paris: Moulin;
1177 1929. 1178
1179 18. Capogrosso V, Gabrieli F, Bellei S, Cartechini L, Cesaratto A, Trcera N, Rosi F,
1180 *Valentini G, Comelli D, Nevin A. An integrated approach based on micro-*
1181 *mapping analytical techniques for the detection of impurities in historical*
1182 *Zn-based white pigments*. *J Anal At Spectrom.* 2015;30(3):828–38. 1183
1184 19. Eastaugh N, Nodolby J, Swiech W. Interpretation of documentary sources
1185 *for the industrial preparation of zinc white in 19th century*. In: Townsend
1186 *JH, Nodolny J, Eyb-Green S, Neven S, Kroustallis S, editors. Dubois H. New*
1187 *York: Making and Transforming Art: Technology and Interpretation; 2014.*
1188 *p. 102–8.* 1189
1190 20. Morley-Smith CT. The development of anti-chalking French process zinc
1191 *oxide*. *J Oil Colour Chem Assoc.* 1950;33:484–501. 1192
1193 21. Rogala DV. Everything old is new again: revisiting a historical symposium
1194 *on zinc oxide paint Films*. In: Keune K, Noble P, Van Loon A, Hendriks E,
1195 *Centeno SA, Osmond G, editors. Metal soaps in art: conservation and*
1196 *research*. Cham: Springer; 2019. p. 317–30. 1197
1198 22. van den Berg KJ, Bonaduce I, Burnstock A, Ormsby B, Scharff M, Heyden-
1199 *reich G, Keune K, editors. Conservation of modern oil paintings*. Cham:
1200 *Springer International Publishing; 2019.* 1201
1202 23. Casadio F, Keune K, Noble P, Van Loon A, Hendriks E, Centeno SA, Osmond
1203 *G, editors. Metal soaps in art: conservation and research*. Cham: Springer;
1204 2019. 1205
1206 24. Sands S. Zinc oxide: warnings, cautions, and best practices. In: *Just Paint.*
1207 *Published by Golden Artist Colors, Inc. 2018. [https://justpaint.org/zinc-](https://justpaint.org/zinc-oxide-warnings-cautions-and-best-practices/)*
1208 *oxide-warnings-cautions-and-best-practices/*. Accessed 19 Oct 2023. 1209
1210 25. Hageraats S, Keune K, Réfrégiers M, van Loon A, Berrie B, Thoury M.
1211 *Synchrotron Deep-UV photoluminescence imaging for the submicro-*
1212 *meter analysis of chemically altered zinc white oil paints*. *Anal Chem.*
1213 *2019;91(23):14887–95.* 1214
1215 26. Izzo FC, Kratter M, Nevin A, Zendiri E. A critical review on the analysis of
1216 *metal soaps in oil paintings*. *ChemistryOpen.* 2021;10(9):904–21. 1217
1218 27. Andersen CK, Taube M, Vila A, Baadsgaard E. Zinc, Paint loss and Harmony
1219 *in blue: degradation problems in Peder Severin Krøyer's paintings and*
1220 *the possible role of zinc white*. *Perspective.* 2016; 1–16. 1221
1222 28. Osmond G, Keune K, Boon J. A study of zinc soap aggregates in a late
1223 *19th century painting by R.G. rivers at the Queensland art gallery*. *AICCM*
1224 *Bull.* 2005;29:37–46. 1225
1226 29. Hermans JJ, Keune K, van Loon A, Stols M, Corkery RW, ledema PD. The
1227 *synthesis of new types of lead and zinc soaps: A source of information for*
1228 *the study of oil paint degradation*. In: Bridgland J, editor, *ICOM-CC 17th*
1229 *Triennial Conference preprints, Melbourne, 15 – 19 September 2014, art.*
1230 *1603, International Council of Museums, Paris. 2014. p. 1–8.* 1231
1232 30. Hermans JJ, Keune K, van Loon A, ledema PD. An infrared spectroscopic
1233 *study of the nature of zinc carboxylates in oil paintings*. *J Anal At Spec-*
1234 *trum.* 2015;30(7):1600–8. 1235
1236 31. Osmond G. Zinc white and the influence of paint composition for stabil-
1237 *ity in oil based media*. In: van den Berg KJ, Burnstock A, de Keijzer M,
1238 *Krueger J, Learner T, Tagle A, Heydenreich G, editors. Issues in contempo-*
1239 *rary oil paint*. Cham: Springer; 2014. p. 263–81. 1240
1241 32. Hermans JJ, Osmond G, van Loon A, ledema P, Chapman R, Drennan
1242 *J, Jack K, Rasch R, Morgan G, Zhang Z, Monteiro M, Keune K. Electron*
1243 *microscopy imaging of zinc soaps nucleation in oil paint*. *Microsc Microa-*
1244 *nal.* 2018;24(3):318–22. 1245
1246 33. Baij L, Chassouant L, Hermans JJ, Keune K, ledema PD. The concen-
1247 *tration and origins of carboxylic acid groups in oil paint*. *RSC Adv.*
1248 *2019;9(61):35559–64.* 1249
1250 34. Hermans JJ, Helwig K. The identification of multiple crystalline
1251 *zinc soap structures using infrared spectroscopy*. *Appl Spectrosc.*
1252 *2020;74(12):1505–14.* 1253
1254 35. Hermans JJ, Helwig K, Woutersen S, Keune K. Traces of water catalyze zinc
1255 *soap crystallization in solvent-exposed oil paints*. *Phys Chem Chem Phys.*
1256 *2023;25(7):5701–9.* 1257

- 1237 36. Clementi C, Rosi F, Romani A, Vivani R, Brunetti BG, Miliani C. Photoluminescence properties of zinc oxide in paints: a study of the effect of self-absorption and passivation. *Appl Spectrosc*. 2012;66(10):1233–41. 1306
- 1238 37. Morley-Smith CT. Zinc oxide - a reactive pigment. *J Oil Col*. 1958;41:85–97. 1307
- 1239 38. Artesani A, Bellei S, Capogrosso V, Cesaratto A, Mosca S, Nevin A, Valentini G, Comelli D. Photoluminescence properties of zinc white: an insight into its emission mechanisms through the study of historical artist materials. *Appl Phys A*. 2016;122(12):1053. 1308
- 1240 39. Artesani A, Dozzi MV, Toniolo L, Valentini G, Comelli D. Experimental study on the link between optical emission, crystal defects and photocatalytic activity of artist pigments based on zinc oxide. *Minerals*. 2020;10(12):1129. 1309
- 1241 40. Hageraats S. Developing microchemical imaging for the study of pigment degradation in oil paint. Doctoral thesis, University of Amsterdam. 2021. 1310
- 1242 41. Salvant Plissin J, de Viguier L, Tahroucht L, Menu M, Ducouret G. Rheology of white paints: how Van Gogh achieved his famous impasto. *Colloids Surf, A*. 2014;458:134–41. 1311
- 1243 42. Janas A, Mecklenburg MF, Fuster-López L, Kozłowski R, Kékicheff P, Favier D, Krarup Andersen C, Scharff M, Bratasz L. Shrinkage and mechanical properties of drying oil paints. *Heritage Science*. 2022;10(1):181. 1312
- 1244 43. Osmond G. Zinc oxide-centred deterioration of modern artists' oil paint and implications for the conservation of twentieth century paintings. Doctoral thesis, The University of Queensland. 2014. 1313
- 1245 44. Shimadzu Y, Keune K, van den Berg KJ, Boon JJ, Townsend JH, Boon JJ. The effects of lead and zinc white saponification on surface appearance. In: *ICOM-CC 15th Triennial Meeting preprints volume II*, New Delhi, 22–26 September 2008. Allied publishers. 2008. p. 626–632. 1314
- 1246 45. Nicolas A. Réflexions sur le portrait dans l'œuvre de Hans Holbein le Jaune. Le "Portrait de la famille du peintre" des beaux-arts de Lille, copie ou réplique peinte sur parchemin de remploi marouflé sur bois : propositions de conservation-restauration et d'une méthode d'analyse de support (Reflections on the portrait in the work of Hans Holbein the Young. The "Portrait of the painter's family" from the Lille Fine Arts Museum, copy or replica painted on replacement parchment mounted on wood: proposals for conservation-restoration and a method for analyzing the support). In French. *Heritage Restorer Diploma-Painting Specialty*, Institut National du Patrimoine, France. 2002. 1315
- 1247 46. Standeven HAL. Oil-based house paints from 1900 to 1960: an examination of their history and development, with particular reference to Ripolin enamels. *J Am Inst Conserv*. 2013;52(3):127–39. 1316
- 1248 47. Kokkori M, Casadio F, Boon JJ. A comprehensive study of early 20th-century oil-based enamel paints: Integrating industrial technical literature and analytical data. In: *Bridgland J, editor, ICOM-CC 17th Triennial Conference preprints*, Melbourne, 15–19 September 2014, art. 0101, International Council of Museums, Paris. 2014. p. 1–8. 1317
- 1249 48. Casadio F, Rose V. High-resolution fluorescence mapping of impurities in historical zinc oxide pigments: hard X-ray nanoprobe applications to the paints of Pablo Picasso. *Appl Phys A*. 2013;111(1):1–8. 1318
- 1250 49. Zhang M, Averseng F, Haque F, Borghetti P, Krafft JM, Baptiste B, Costentin G, Stankic S. Defect-related multicolour emissions in ZnO smoke: from violet, over green to yellow. *Nanoscale*. 2019;11:5102–15. 1319
- 1251 50. Otero V. Historically accurate reconstructions of Amadeo's chrome yellows: an integrated study of their manufacture and stability. Doctoral thesis, Universidade Nova de Lisboa. 2018. 1320
- 1252 51. Christiansen MB, Baadsgaard E, Sanyova J, Simonsen KP. The artists' materials of P. S. Krøyer: an analytical study of the artist's paintings and tube colours by Raman, SEM-EDS and HPLC. *Heritage Sci*. 2017;5:39. 1321
- 1253 52. Muir K, Langley A, Bezur A, Casadio F, Delaney J, Gautier G. Scientifically investigating Picasso's suspected use of Ripolin house paints in still life, 1922 and The Red Armchair, 1931. *J Am Inst Conserv*. 2013;52(3):156–72. 1322
- 1254 53. Doherty S. Expand Your Options by Adding Zinc White Gouache to Transparent Watercolors. In: *Artists Network*. 2007. <https://www.artistsnetwork.com/art-mediums/mixed-media/expand-your-options-by-adding-zinc-white-gouache-to-transparent-watercolors/>. Accessed 19 Oct 2023. 1323
- 1255 54. Richard P. Sennelier, l'artisan des couleurs (Sennelier, a history in color). In French/English. Editions du Chêne. 2012. 1324
- 1256 55. Hopper E. Ledger books, record of the work of Edward Hopper. New York: Whitney Museum of American Art Books II-II; 1984. 1325
- 1257 56. Pichon L, Calligaro T, Gonzalez V, Lemasson Q, Moignard B, Pacheco C. Implementation of ionoluminescence in the AGLAE scanning external microprobe. *Nucl Instrum Methods Phys Res, Sect B*. 2015;348:68–72. 1326
- 1258 57. Altomare A, Corriero N, Cuocci C, Falcicchio A, Moliterni A, Rizzi R. QUALX2.0: a qualitative phase analysis software using the freely available database POW-COD. *J Appl Crystallogr*. 2015;48:598. 1327
- 1259 58. Cotte M, Gonzalez V, Vanmeert F, Monaco L, Dejoie C, Burghammer M, Huder L, de Nolf W, Stuart F, Fazlic I, Chaffetou C, Wallez G, Jiménez N, Albert-Tortosa F, Salvadó N, Possenti E, Colombo C, Ghirardello M, Comelli D, Avranovich Clerici E, Vivani R, Romani A, Costantino C, Janssens K, Taniguchi Y, McCarthy J, Reichert H, Susini J. The "Historical Materials BAG": a new facilitated access to synchrotron x-ray diffraction analyses for cultural heritage materials at the European synchrotron radiation facility. *Molecules*. 2022;27(6):1997. 1328
- 1260 59. Chaffetou C, Costantino C, Iacconi C, Vanmeert F, Fazlic I, Monaco L, Cotte M, Ghirardello M, Palladino N, Gonzalez V. Structural Analysis of Historical Materials. *Eur Synchrotron Radiat Facil*. 2024. <https://doi.org/10.1515/ESRF-ES-515931562>. 1329
- 1261 60. Riminesi C, Villalobos Portillo EE, Possenti E, Beauvoit E, Avranovich Clerici E, Vanmeert F, Broers FTH. Structural Analysis of Historical Materials. *European Synchrotron Radiation Facility*. 2025. <https://doi.org/10.1515/ESRF-ES-658022426>. 1330
- 1262 61. Dumazet A, De Mecquenem C, Theron, Chalmin E, Beauvoit E, Avranovich Clerici E, Albert-Tortosa F. Structural Analysis of Historical Materials. *European Synchrotron Radiation Facility*. 2025. <https://doi.org/10.1515/ESRF-ES-945457975>. 1331
- 1263 62. Roisnel T, Rodriguez-Carvajal J. WinPLOTR: a Windows powder diffraction patterns analysis tool. *Mater Sci Forum*. 2001;378–381:118–23. 1332
- 1264 63. Artesani A. Time-Resolved Photoluminescence in conservation science: study of crystal defects as markers of modern semiconductor pigments and of their degradation. Doctoral thesis, Politecnico di Milano. 2019. 1333
- 1265 64. Coulier PJ. Question de la cèruse et du blanc de zinc : envisagée sous les rapports de l'hygiène et des intérêts publics (The issue of lead white and zinc white: considered from hygiene and public interest perspective). Paris: J.-B. Baillière; 1852. 1334
- 1266 65. Standage HC. The artists' manual of pigments: showing their composition, non-permanency, and adulterations, effects in combination with each other and with vehicles, and the most reliable tests of purity : together with the Science and Art Department's examination questions on painting. Crosby Lockwood and Co., London. 1887. 1335
- 1267 66. Holley CD. The lead and zinc pigments. Hoboken: Wiley; 1909. 1336
- 1268 67. Haddad A, Rogge CE, Martins A, Dijkema D. "Foundations of a great metaphysical style": unraveling Giorgio de Chirico's early palette. *Heritage Sci*. 2022;10(1):70. 1337
- 1269 68. Bonaduce I, Duce C, Lluveras-Tenorio A, Lee J, Ormsby B, Burnstock A, van den Berg KJ. Conservation issues of modern oil paintings: a molecular model on paint curing. *Acc Chem Res*. 2019;52(12):3397–406. 1338
- 1270 69. Zhang M, Averseng F, Krafft JM, Borghetti P, Costentin G, Stankic S. Controlled formation of native defects in ultrapure ZnO for the assignment of green emissions to oxygen vacancies. *J Phys Chem C*. 2020;124(23):12696–704. 1339
- 1271 70. Artesani A, Gherardi F, Mosca S, Alberti R, Nevin A, Toniolo L, Valentini G, Comelli D. On the photoluminescence changes induced by ageing processes on zinc white paints. *Microchem J*. 2018;139:467–74. 1340
- 1272 71. Eastaugh N, Walsh V, Chaplin T, Siddall R, editors. *The pigment compendium: a dictionary of historical pigments*. Oxford: Elsevier Butterworth-Heinemann; 2004. 1341
- 1273 72. Macchia A, Cesaro SN, Keheyani Y, Ruffolo SA, La Russa MF. White zinc in linseed oil paintings: chemical, mechanical and aesthetic aspects. *Periodico di Mineralogia*. 2015;84(3):30–43. 1342
- 1274 73. Vieille Montagne, editor. *Blanc de zinc (Zinc white)*. Booklet edited by La Société de La Vieille Montagne. In French. After 1920. 1343
- 1275 74. Hageraats S, Keune K, Stankic S, Stanescu S, Tromp M, Thoury M. X-ray nanospectroscopy reveals binary defect populations in sub-micrometric ZnO crystallites. *J Phys Chem C*. 2020;124(23):12596–605. 1344
- 1276 75. Martins A, Albertson C, McGlinchey C, Dik J. Piet Mondrian's Broadway Boogie Woogie: non invasive analysis using macro X-ray fluorescence mapping (MA-XRF) and multivariate curve resolution-alternating least square (MCR-ALS). *Heritage Sci*. 2016;4:22. 1345

1375 76. Govindaraju K, Roelandts I. Compilation report on trace elements in six
 1376 anrt rock reference samples: diorite Dr-N, Serpentine Ub-N, Bauxite Bx-N,
 1377 Disthene Dt-N, Granite Gs-N and Potash Feldspar Fk-N. *Geostand Newsl.*
 1378 1989;13(1):5–67.
 1379 77. Palamara E, Das PP, Nicolopoulos S, Tormo Cifuentes L, Kouloumpi E,
 1380 Terlixi A, Zacharias N. Towards building a Cathodoluminescence (CL)
 1381 database for pigments: characterization of white pigments. *Heritage Sci.*
 1382 2021;9(1):100.
 1383 78. Stoecklein W, Göbel R. Application of cathodoluminescence in paint
 1384 analysis. *Scanning Microsc.* 1992;6(3):4.
 1385 79. Kadikova I, Pisareva SA, Grigorieva IA, Lukashova M. Pigments of soviet
 1386 Artists in the 1950s – Late 1970s. In: van den Berg KJ, Bonaduce I, Burn-
 1387 stock A, Ormsby B, Scharff M, Carlyle L, Heydenreich G, Keune K, editors.
 1388 Conservation of modern oil paintings. Cham: Springer; 2019. p. 165–89.
 1389 80. Palladino N, Guillemot H, Marcos Alvarez E, Salvant J. Les peintures au
 1390 blanc de zinc : du minerai à la palette (Zinc white paints: from the mineral
 1391 to the palette). In French. *Technè*. Submitted in November 2023.

Publisher’s Note

1392 Springer Nature remains neutral with regard to jurisdictional claims in pub-
 1393 lished maps and institutional affiliations.
 1394

REVISED PROOF

Submit your manuscript to a SpringerOpen® journal and benefit from:

- ▶ Convenient online submission
- ▶ Rigorous peer review
- ▶ Open access: articles freely available online
- ▶ High visibility within the field
- ▶ Retaining the copyright to your article

Submit your next manuscript at ▶ [springeropen.com](https://www.springeropen.com)

Journal : BMCTwo 40494	Dispatch : 10-12-2023	Pages : 31
Article No : 1082	<input type="checkbox"/> LE	<input type="checkbox"/> TYPESET
MS Code :	<input checked="" type="checkbox"/> CP	<input checked="" type="checkbox"/> DISK